1-1-2005

Measurement of Lipid Peroxidation in Biology Models Using Gas-Chromatography-Mass Spectrometry

Madhavi Lokireddy

APPROVAL

Measurement of Lipid Peroxidation in Biological models

Using Gas-chromatography-Mass Spectrometry

By

Madhavi Lokireddy

APPROVED

Director: Dr. Steven Pernecky

Signature:

Date:

Committee Member: Dr. Heather Holmes

Signature:

Date:

Committee Member: Dr. Hedeel Guy Evans

Signature:

Date:

Department Head: Dr. Maria Milletti

Signature:

Date:

Dean of Graduate Studies and Research: Dr. Robert Holkeboer

Signature

Date:

ACKNOWLEDGEMENTS

I would like to take this opportunity to thank my research advisor, Dr. Steven Pernecky. He has been a great source of guidance, motivation, and patience. His leadership in scientific endeavors has been an inspiration to me throughout my graduate career, and I am grateful for having had the opportunity to pursue my master's degree under his supervision.

I would like to express my deepest appreciation to my committee members, Dr. Heather Holmes and Dr. Heedel Evans, for their assistance and encouragement. Myoblast cells were a kind gift from Dr. Mc Gregor, and I would like to express my sincere gratitude for that. I also would like to thank Dr. Basu for the methodology development and his wise input throughout the project.

I sincerely appreciate my graduate advisor, Dr. Krishnaswamy Rengan, for his endless support, encouragement, and assistance throughout the program. I have been blessed with the financial support during my graduate career and acknowledge Eastern Michigan University for providing a research assistantship. I would also like to thank department heads Dr. Wade Tornquist and Dr. Maria Milletti for their support and encouragement. My acknowledgements would be left incomplete without mentioning my friends for their help and encouragement during my stay at Eastern Michigan University. Finally, I would like to thank my husband for his unending support and cooperation. I am so grateful for my son, who always brings a little joy into a long day, for his patience and finally, I am thankful to all who have made this journey both possible and pleasurable.

ABSTRACT

C2C12 mouse myoblast cells, grown in glass vials, were connected to a cryofocusing unit to trap volatile organic compounds (VOCs). The VOCs were eluted from the trap by capacitive discharge into a gas chromatograph with time-of-flight mass spectral capabilities (GC-TOFMS) and were found to include the lipid peroxidation product hexanal. The pro-oxidant cumene hydroperoxide elevated the levels of these lipid peroxidation products, whereas the anti-oxidant butylated hydroxy toluene (BHT) impaired their production. Derivatization of the aldehyde products of lipid peroxidation in the same myoblast cells with pentafluorobenzyl hydroxylamine hydrochloride (PFB) provided evidence for formation of non-volatile products of lipid peroxidation such as malondialdehyde and 4hydroxynonenal.

Similar experiments with the human tracheal epithelial cells, 9-HTE cells treated with *Haemophilus influenza* bacteria, showed elevated levels of malondialdehyde at 8-hour incubation time intervals giving the initial evidence that the products of lipid peroxidation are formed long before the COX-1 enzyme is activated.

TABLE OF CONTENTS

LIST OF FIGURES

Measurement of Lipid Peroxidation in Biological Models Using Gas-chromatography-Mass Spectrometry

By

Madhavi Lokireddy

Thesis

Submitted to the Department of Chemistry

Eastern Michigan University

In partial fulfillment of the requirements

for the degree of

MASTER OF SCIENCE

in

Chemistry

December 2005

Ypsilanti, Michigan

INTRODUCTION

1.1 Lipids and polyunsaturated fatty acids

Lipids are a large and diverse group of naturally occurring organic compounds defined on the basis of their solubility rather than on their structure. They are insoluble in water but soluble in nonpolar solvents. In biological systems they play an important role as structural components of the lipid bilayer and as functional components in signaling pathways. The lipids of all higher organisms contain substantial quantities of polyunsaturated fatty acids (PUFA). Two principle families of polyunsaturated fatty acids occur in nature, and they are derived biosynthetically from linoleic (9-cis, 12-cis octadecadienoic) and α-linolenic (9-cis, 12-cis, and 15-cis-octadecatrienoic) acids. Structures of linoleic acid and α-linolenic are shown in Figure 1.

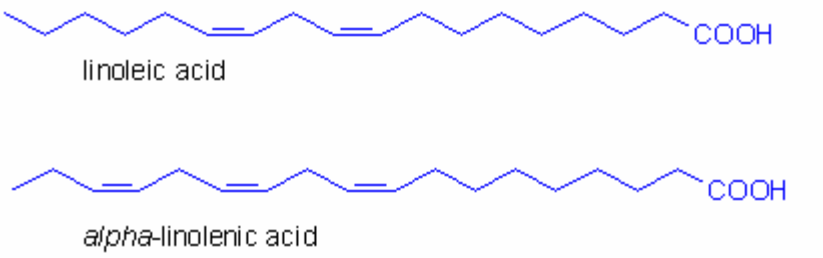

Figure 1. Structures of linoleic and α-linolenic acids [1].

In light of the fact that these fatty acids are synthesized in plants but not in animal tissues, they are therefore essential dietary components in animals. Polyunsaturated fatty acids can be found in most lipid classes, but they are especially important as the constituents of the phospholipids, where they appear to confer distinctive properties to

the membranes, one of which is to promote fluidity of the cell membrane [2]. Polyunsaturated fatty acids are divided into three main families designated as n-3, n-6, and n-9, classified on the basis of the location of the double bond from the terminal methyl group. α-Linolenic acid, 11,14,17- eicosatrienoic acid, stearidonic acid, 3,6,9,12,15- octadecapentaenoic acid are members of the n-3 family. Linoleic acid, γ-linolenic acid, 8-cis,-11-cis, 4-cis-eicosatrienoic acid, and arachidonic acid belong in the n-6 family. The primary PUFA in the n-9 family is 5,8,11-eicosatrienoic acid.

1.2 Lipid bilayer

The lipid bilayer that comprises cell membranes is principally composed of phophatidylcholine, whose structure is shown in Figure 2. The polar, hydrophilic head group of the lipid bilayer is water soluble, containing a negatively charged phosphate group and a positively charged nitrogen group designated as choline. The nonpolar, hydrophobic tail points toward the middle of the bilayer, and the hydrophilic groups point both toward the outer and inner surfaces of the membranes [3].

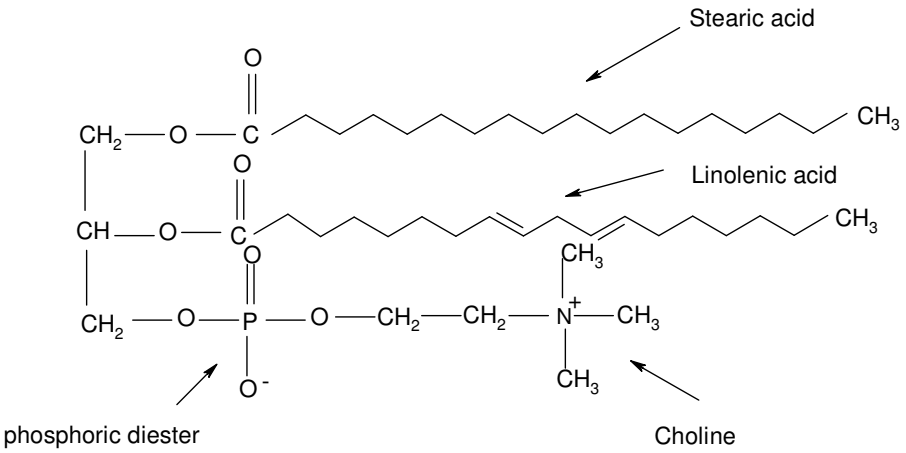

Figure 2. Structure of a phosphatidylcholine.

Arachidonic acid is a polyunsaturated fatty acid that contains four cis double bonds, is normally present at the sn-2 position in phospholipid, as shown in Figure 3, is an essential component of the membrane [4]. The double bonds give arachidonic acid flexibility and the capacity to react with molecular oxygen.

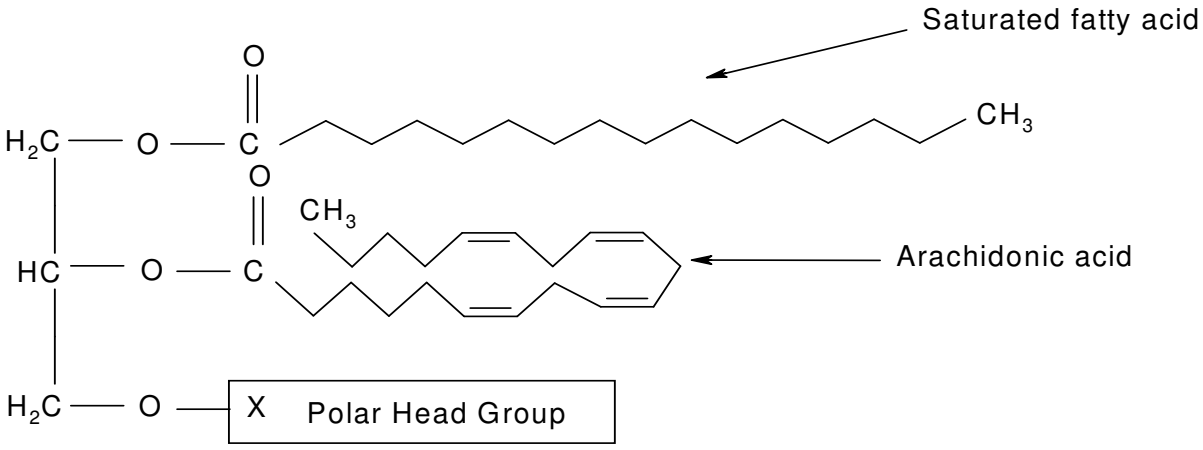

Figure 3. Structure of membrane phospholipid

1.3 Metabolic fates of PUFA

Most of the unsaturated fatty acids occurring in the human body undergo one of three types of metabolic processes depending upon the circumstances and the environmental conditions: β-oxidation, oxidative decomposition, or enzymatic decomposition.

1.3. a. β-oxidation

Unsaturated fatty acids are ultimately metabolized to acetyl CoA in the β-oxidation pathway. However, polyunsaturation or unsaturation at odd-numbered carbon positions of the acyl-CoA will produce a molecule that the major pathway cannot

utilize as a substrate [5]. Various enzymes exist in the peroxisome to convert these molecules to appropriate intermediates, which can be then shuttled into the normal pathway as shown in Figure 4.

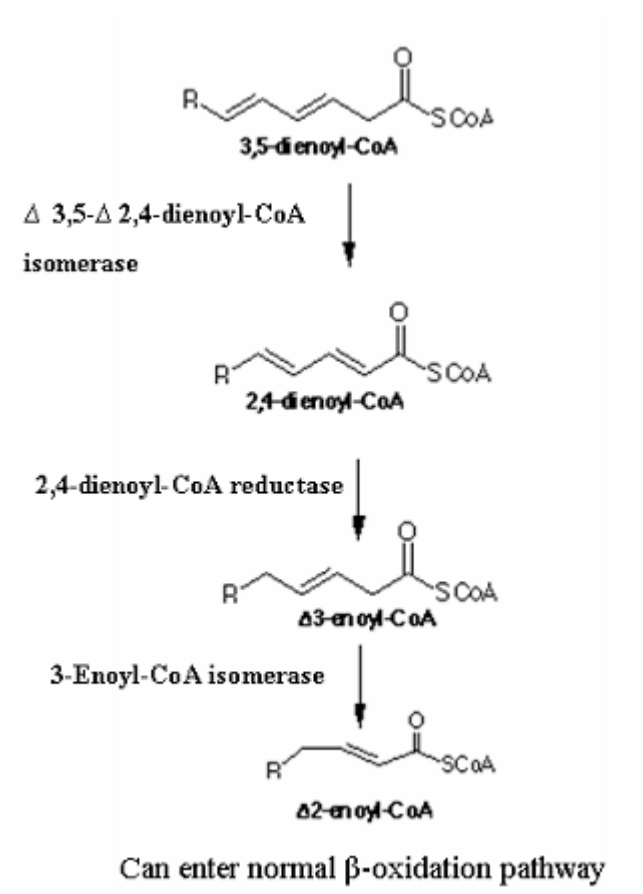

Figure 4. Oxidation of odd-numbered polyunsaturated fatty acids [6].

Certain types of PUFA may enter the β-oxidation spiral and produce a Δ3,5-dienoyl-CoA. This product is unable to enter the normal β-oxidation spiral because the acyl-CoA oxidase adds a double bond at the 2 position, but cannot do this because of the double

bond at the 3 position; therefore, Δ3,5-Δ2,4-dienoyl-CoA isomerase converts the Δ3,5-dienoyl-CoA to a 2,4-dienoyl-CoA [7]. The 2,4-dienoyl-CoAs may exist naturally and are also produced during the breakdown of PUFA. These molecules are also unable to enter the major β-oxidation spiral. To combat this problem, 2,4-dienoyl-CoA reductase converts the 2,4-dienoyl-CoA into a 3-enoyl-CoA [8]. The 3-enoyl-CoAs are produced by the normal β-oxidation of odd-position unsaturated fatty acids, as well as through the breakdown of PUFA. The Δ3-enoyl-CoA is converted to a Δ2-enoyl-CoA, a molecule that is an intermediate of the normal β-oxidation spiral [9].

1.3. b. Oxidative decomposition products of PUFA

Lipid peroxidation (LPO) is a free radical chain process that occurs either by thermal or photochemical homolytic cleavage of an RH bond or by hydrogen atom abstraction from polyunsaturated fatty acids (PUFA). In the final stages of oxidation, the peroxyl radicals decompose to form aldehydes such as hexanal, pentanal, propanal, malondialdehyde, alkanes, hydroxyl-alkenals, and fatty acid alcohols. The basic reaction sequence of lipid peroxidation pathway is shown in Figure 5.

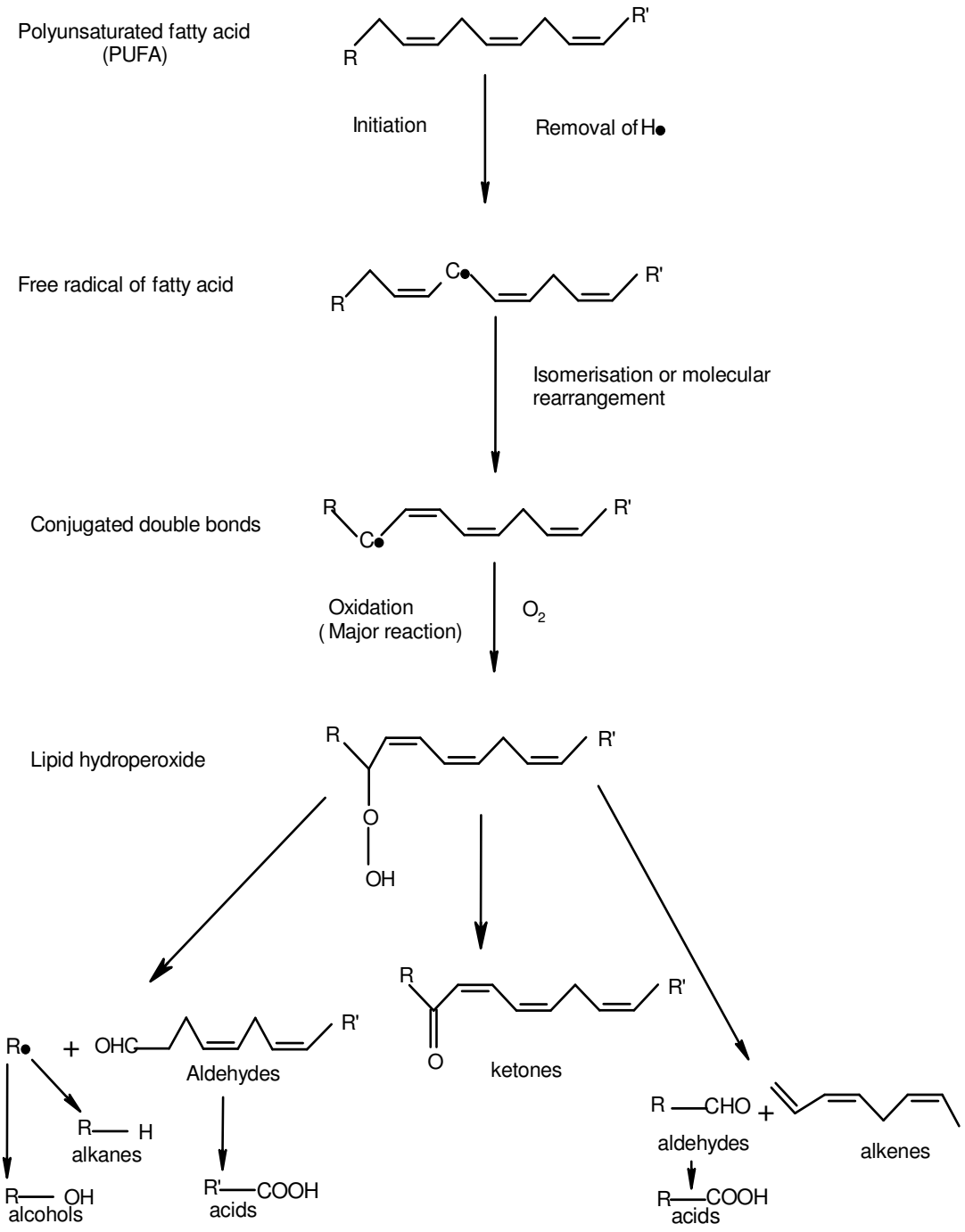

Figure 5. General pathway of the formation of lipid peroxidation products [10].

Cellular membrane lipids are the major targets of oxidative damage [11]. Their unstable, reactive double bonds make them susceptible to oxidative attack, which leads to a chain reaction of lipid peroxidation. Lipid peroxidation, in general, is well known to produce many reactive species that are biologically detrimental. Among several reactive lipid aldehydes, 4-hydroxy-2-nonenal (HNE) and 4-hydroxyhexanal (HHE) have drawn the most research interest in recent years [12]. Because of their stability and high reactivity, lipid aldehydes are known to be involved in various pathophysiological processes associated with oxidative stress, and they also influence membrane fluidity [13]. Rahman et al [14] stated that the lipid aldehyde, 4-HNE, can be produced from arachidonic acid, linoleic acid, or their hydroperoxides in concentrations of 1 μM to 5 mM, in response to oxidative insults and is believed to be responsible for many of the effects during oxidative stress *in vivo*.

1.3. c. PUFA oxidation without structural decomposition

The enzymic formation of oxidized lipids involves the stereospecific addition of molecular oxygen to a PUFA (polyunsaturated fatty acid). For example, prostaglandins (PGs) and leukotrienes are formed by cyclo-oxygenases and lipoxygenases metabolizing arachidonic acid [14,15]. Arachidonic acid is converted into PGG_2 and PGH_2 by cyclo-oxygenase1. Both of these products are highly unstable and are transformed into a variety of bioactive products, including PGE_2, PGD_2, PGF_2, thromboxane A2, and prostacyclin, which play an essential role in the inflammatory response [15].

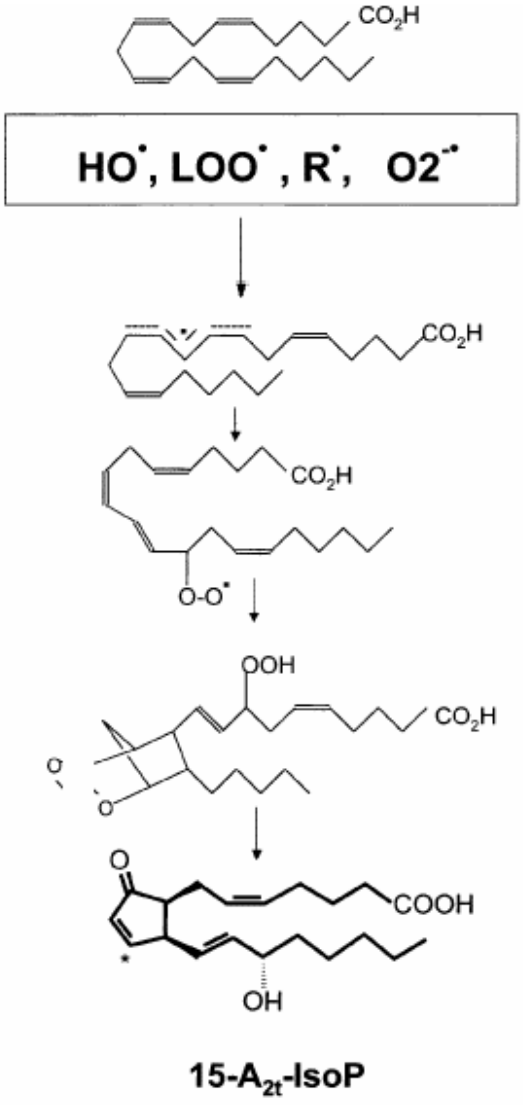

Figure 6. Formation of a prostaglandin-like molecule in a non-enzymatic pathway [16].

The lipoxygenases also control the lipid peroxidation reaction to form hydroperoxide products that can be converted into the highly active leukotrienes, which also play a role in the inflammatory response [17]. Both cyclo-oxygenase and lipoxygenases require low levels of lipid peroxide that are already present in PUFAs to catalyze their reactions. It has been known that the non-enzymatic oxidation of PUFA

results in products that are structural analogues of those that are formed enzymatically [19], and is shown in Figure 6. It is fascinating to note that during the peroxidation process, the PUFA is converted from lipid peroxide into electrophile-containing lipids, (Figure 6.) such as 15-A_{2t}-IsoP (isoprostane) and HNE. The biological significance of this reaction was first discovered from non-enzymatic decomposition of arachidonic acid to form the family of compounds known as the isoprostanes [18]. Isoprostanes exert unique biological effects that include vasoconstriction in the kidney after traumatic release of myoglobin into the circulation in a process known as rhabdomyolosis [19].

1.4 Toxicological/ Physiological affects of lipid peroxidation

Lipid peroxidation products are more stable than free radicals so they can directly or indirectly affect many functions of organs. They can initiate gene transcription, affect the immune system, initiate fibrosis or inflammation, and inactivate thiol-containing enzymes [20].

Lipid peroxidation has been linked with various pathological conditions such as atherosclerosis, myocardial infarction, and carcinogenesis, postischemic reperfusion injury, mammography dysplasia, chronic gastritis, and precancerous dysplasia [21]. Aldehydes from lipid peroxidation such as malonaldehyde and 4-hydroxynonenal have been shown to be cytotoxic and genotoxic [22-25]. Lipid peroxidation has also been implicated as the cause of severe health problems such as renal failure, heart disease, liver disease, cancer, and diabetes [21].

1.5 Measurement of lipid peroxidation production cell systems

Various approaches that can be utilized to assess lipid peroxidation products are shown in Figure 7. These techniques have distinct advantages and disadvantages under different circumstances and employ a combination of complementary techniques [20]. The extent of lipid peroxidation has been measured by various methods including the analysis of lipid hydroperoxides [21], conjugated dienes [22, 24], reactive aldehydes [24-26], and of hydrocarbons in exhaled air [27, 28]. A widely used index of peroxidation is the measurement of the secondary product, malonaldehyde (MDA) by thiobarbituric acid assay. However, due to the uncertainty in the structure of the derivative and the lack of specificity of the assay, the level of MDA is usually expressed as thiobarbituric acid reactive substances (TBARS). This assay is hindered by possible reactivity of other aldehydes with TBA and the harsh conditions used in sample preparation. These problems have sometimes led to inconclusive results and may lead to misinterpretation of data; thus the thiobarbituric acid assay was not employed in this study.

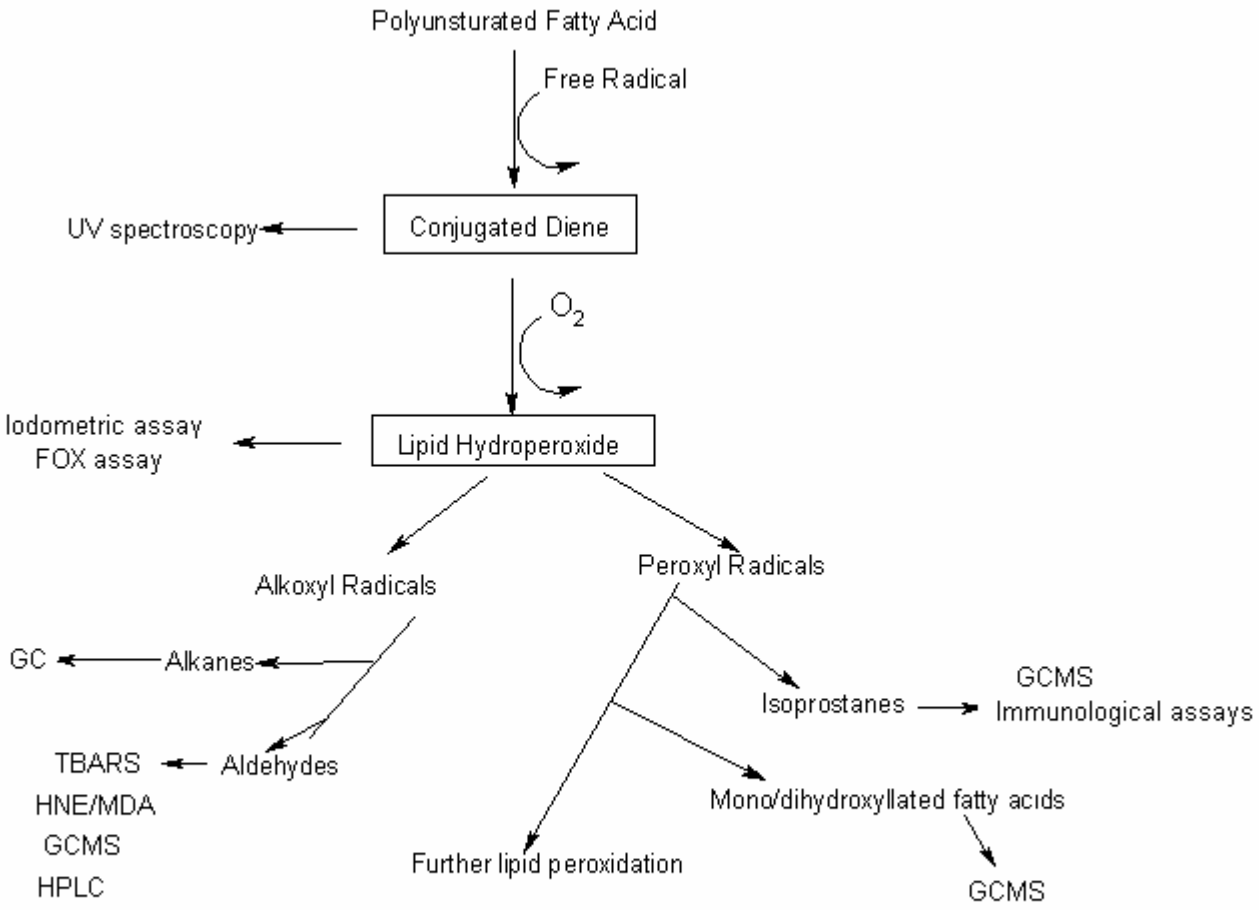

Figure 7. Different methods for the measurements of lipid peroxidation products [27].

1.6 Gas chromatography

Gas chromatography (GC) has been a powerful tool for the detection, separation, and identification of volatile and semi-volatile organic compounds. The most important advantage of GC is that it can be used for rapid, yet complete, analysis of a mixture of compounds over a wide range of concentrations with excellent precision and accuracy [28,29].

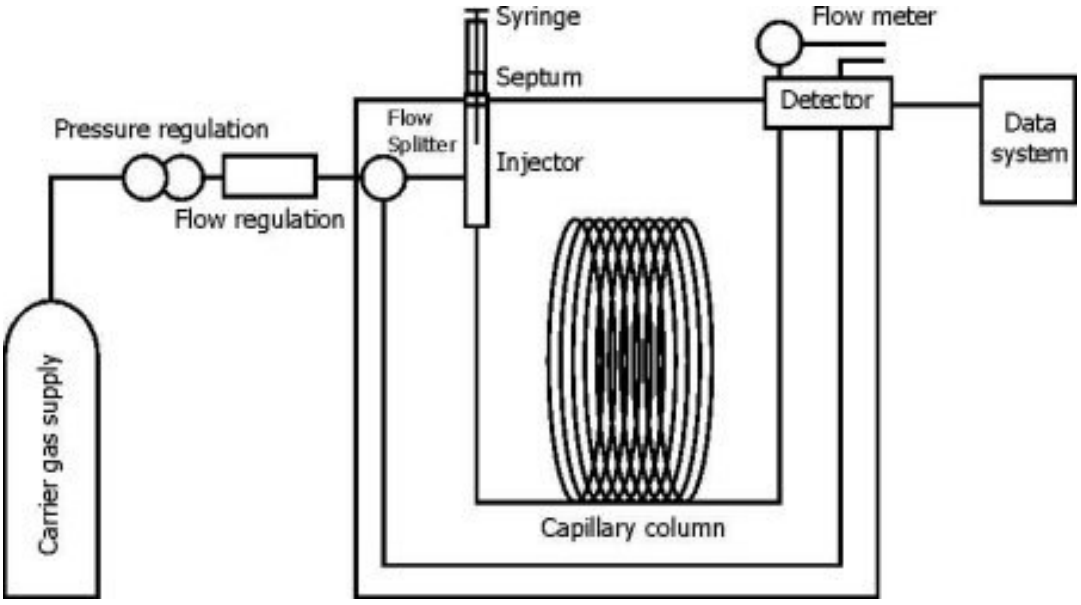

Figure 8. Schematic diagram of a typical gas chromatograph [29].

A typical gas chromatogram is shown in Figure 8, which consists of carrier gas, flow controller, a column, an oven in which the column is placed, an injector port, a detector, and a recorder. In a gas chromatographic analysis, small amounts of sample are injected into a moving stream of carrier gas, which is the mobile phase like nitrogen, helium, and hydrogen gases.

The sample is carried by the stream through a column that consists of a tube containing a stationary phase, which can be a solid or a liquid [30]. Separation of a sample mixture into its individual components is achieved if the components are retained in the column to different extents. The time it takes after sample injection for the analyte peak to reach the detector is called the retention time or t_R. The retention time depends on the affinity of the stationary phase for the component, the temperature, and the rate of flow of the gas.

In GC, two types of columns are used to separate compounds: packed and capillary columns. Column material, internal diameter, and film thickness are important parameters in GC. Packed columns separate the simple mixtures rapidly, but the resolving power for complex mixture is limited. Resolution of peaks can be improved with an increase in the column length, but the analysis time increases proportionally. Capillary columns were first introduced by Golay [31] and now are widely used for the separation and analysis of low molecular weight organic compounds.

1.6.a. Headspace analysis

Static and dynamic headspace techniques have also been used for the analysis of volatile organic compounds [31-34]. Static headspace is a simple technique in which the sample containing the volatile organic compounds is allowed to equilibrate with its headspace gas in a sealed container at a constant temperature. This technique is limited due to high detection limits and also requires thermodynamic equilibrium of the sample. In dynamic headspace analysis (also known as purge and trap), the sample is drawn to a sorbet bed prior to injection to the GC. Heating the trap and then transporting the vapor plug to the gas chromatographic system desorbs the sample. This technique offers good sensitivity and solvent free operation [32, 34]. It can collect volatile organic compounds over a period of time, but the disadvantages include difficulty of use, long preparation and analysis times, and inability to examine a large number of samples quickly.

Frankel and his co-worker described a headspace gas chromatographic method as a rapid, sensitive, and simple method for the determination of volatile organic compounds, such as hexanal, as an indicator of n-6 PUFA peroxidation in rat liver samples and red blood cell membranes of humans [35]. This method can separate and

identify complex mixtures in one-tenth the time of conventional GC, on the order of 60 or less seconds rather than minutes, and is able to distinguish between products of n-6 PUFA (hexanal and pentane) and propanal, which is a product of n-3 PUFA. With a rapid and sensitive capillary gas chromatographic-head space method, it is possible to obtain 15 determinations per hour because cleaning of the injector and trapping system between each sample is not required.

1.6.b. Liquid phase analysis

Analytical methods for biomarkers such as lipid peroxidation products have been developed recently and led to the identification of biomarkers within living systems. These biomarkers are usually activated only when exposure to oxygen radicals has occurred and are quantified long before physiological effects are observed. Chemical derivatization of these molecules is required to improve volatility and stability during analysis by gas chromatography [22]. The current research focused on the use of (2,3,4,5,6-pentafluorobenzyl) hydroxylamine hydrochloride (PFBHA.HCL) to form the pentafluorobenzyl-oxime (PFB-Oxime) derivatives of unsaturated aldehydes, such as 4-hydroxy-non-2-enal (HNE) and MDA, followed by trimethylsilylation of the hydroxyl group to trimethylsilyl (TMS) ethers.

1.7 Mass spectrometry (MS)

Mass spectrometry is an analytical technique that measures the mass-to-charge ratio (m/z) of ions generated by the fragmentation of molecules. The mass spectrum is a plot of the ion abundance as a function of m/z. Sample introduction, sample ionization, separation of ions according to their mass to charge ratio, and ion detection are the four steps in a mass spectrometric analysis.

In a time-of-flight mass spectrometer, the m/z of an ion is determined by measuring its time-of-flight, i.e. its travel time from the ion source to the detector. Because the ions all travel the same distance from the ion source to the detector and they all have essentially the same kinetic energy, their travel time is proportional to $(m/z)^{1/2}$. Thus, ions of different m/z ratios arrive at the detector at different times (separated) depending on their m/z ratios; the heavier the ion, the longer its time-of-flight. Ions created in the ion source are pushed out of the ion source by applying an electrical pulse to the push pulse electrode as shown in Figure 9. The difference in electrical potential accelerates the positively charged ions. All of the ions accelerate almost simultaneously and leave the ion source with essentially the same kinetic energy as shown in Figure 10. After the ions leave the Ion Source, they enter a drift region where their energy remains constant, as shown in Figure 11. Since the ions have almost the same kinetic energy, their velocities depend only on their mass to charge ratio (m/z) as shown in Figure 12.

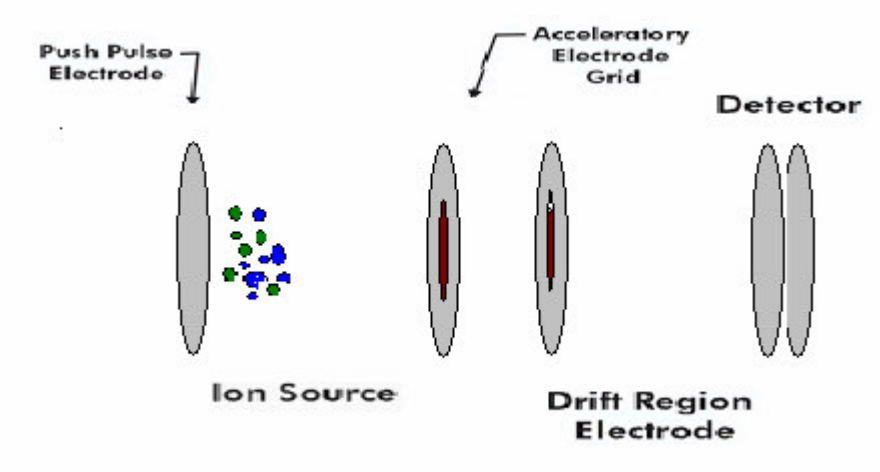

Figure 9. Applying an electrical pulse to the push pulse electrode, ions pushed out of the Ion source.

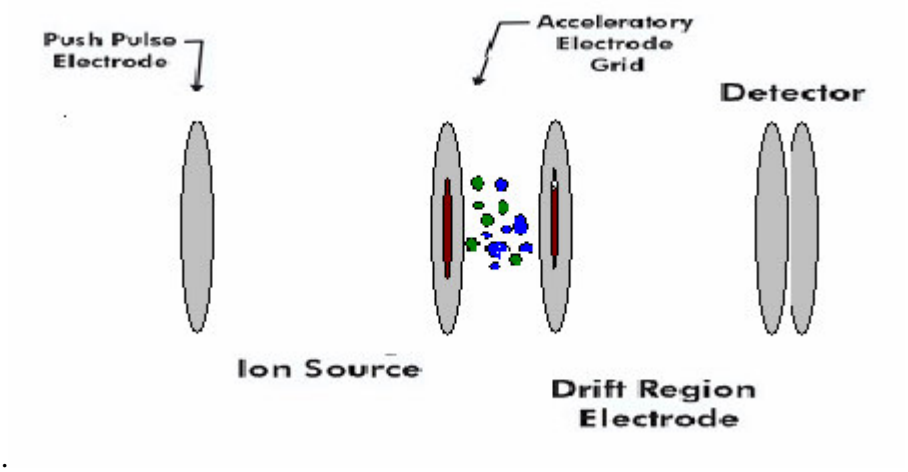

Figure 10. Electrical potential differences create an electrical force for accelerating ions.

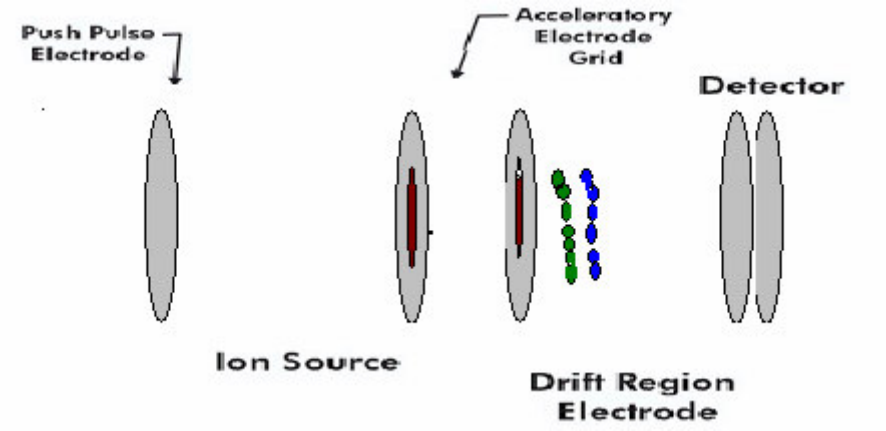

Figure 11. Accelerated ions leave the ion source and separate based on m/z ratio

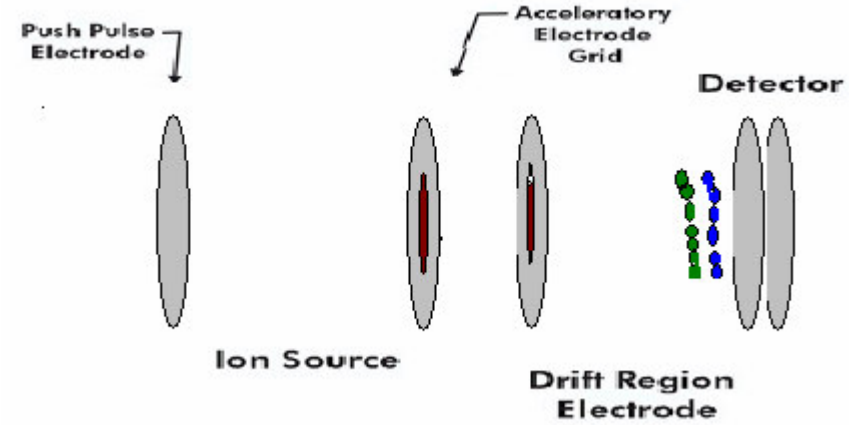

Figure 12. Ions reach the detector separated in time [30].

1.7a. Ion trap/Chemical Ionization (CI) vs electron impact ionization (EI)

Volatile substances can be ionized by electron (impact) ionization (EI) in a process involving the interaction of the gaseous sample with an electron beam generated by a heated filament in the ion source. Chemical ionization (CI) relies on the interaction of molecule of interest with a reactive ionized reagent species [36]. Several investigators have worked on the variable capabilities of EI and CI and stated that these two methods are complementary to each other and that employing a combination of these two methods would help in the identification of the complete profile of lipid peroxidation [10, 20, 28,]. Current research is aimed at identifying the products of lipid peroxidation using these two methods.

1.8 Mammalian cells in determination of lipid peroxidation products

1.8.a. C2C12 Cells

Myoblast are the proliferating cells (immature), which, on fusion with other myoblasts, give rise to more mature nucleated cells called myotubules. Skeletal muscle is seldom considered a primary target of oxidative stress. The irony is that exercise increases the production of free radicals by virtue of an increase in oxygen exploitation. Overall, oxygen radicals and the reactive species that they spawn harm other species with which they come in contact [37]. Cell membranes possess polyunsaturated fatty acids that are highly susceptible to radical assault in the process of lipid peroxidation as described earlier. Several mechanisms have been forwarded to explain the etiology of exercise-induced muscle damage summarized in Figure 13.

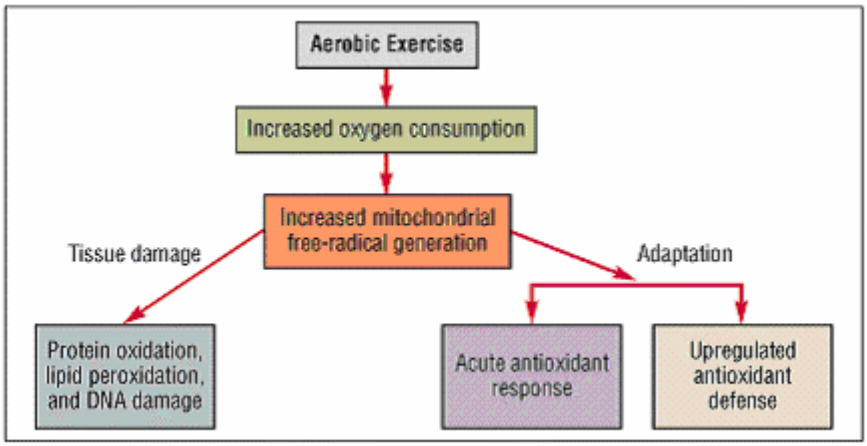

Figure 13. Chronic exercise produces a cascade of events and adaptations that mitigate tissue damage [38]

In the current study, mouse skeletal muscle myoblasts (C2C12) were used to carry out the studies of lipid peroxidation.

1.8 b. 9-HTE cells

Elevated cytokines are always the consequence of proinflammatory responses [39] and are also believed to be the markers of lipid peroxidation. Mucosal epithelial cells act as biological sensors reacting to elevated levels of cytokines as observed in response to microbial pathogens [40]. The current study used the 9-HTE (human tracheal epithelial cells) to measure the lipid peroxidation products in response to nontypeable Haemophilus influenzae (NTHi), a gram-negative bacterial pathogen that exists as a commensal organism in the human nasopharynx. Studies carried out by Clemans et al [40] found that NTHi induces IL-6, IL-8, and TNF-α from 9-HTE cells. Work by Frankel et al [35] showed that proinflammatory cytokines and markers of oxidative stress would

elevate the levels of lipid peroxidation. In the current study, a quantitative measurement of the products of lipid peroxidation using GC/LC-MS by conventional derivatization techniques is employed.

1.9 Research objectives

In this the formation of both volatile and non-volatile products of lipid peroxidation in stimulated myoblast (immature) was compared to that in myotubules (mature). An attempt was also made to identify how the culture conditions influence the measurement of LPO products in 9-HTE cells.

EXPERIMENTAL PROCEDURES

2.1 Cell culture

A mouse myoblast cell line (C2C12, ATCC) was used for this research. The cell suspensions (at about 5 x 10^6 cells) were transferred from a T-75 flask into a 50-mL falcon test tube, and the cells were centrifuged in a Beckmann Centrifuge (Model TJ-6) for 10 minutes at 1000 rpm. The flask was washed with 1% phosphate buffered saline (GIBCO BRL, PBS; containing 2.6 mM potassium chloride, 1.5 mM potassium phosphate, 137 mM sodium chloride, and 15 mM sodium phosphate, anhydrous, pH 7.4) to release adherent cells. Old media was aspirated and the cells were transferred to a 50-mL conical polypropylene tube (Falcon). The cell suspension was centrifuged for 10 minutes at 1000 rpm and PBS was aspirated. The cell pellet was suspended in a small volume of DMEM (GIBCO, Dulbeco's modified eagles medium) and mixed thoroughly by repetitive pipetting. The cells were plated at a density of 1.5 X 10^5 cells/mL in a T-75 flask. The cell suspension was incubated at 37 °C with 5% carbon dioxide for 48 hours. All operations were carried out under a hood to maintain sterile conditions.

2.1. a. Culture medium

Cells were cultured in 450 mL of RPMI1640 (GIBCO-BRL) medium with 50 mL of 10% heat-inactivated fetal bovine serum (Hyclone), 450 µL of 0.1 mM β-mercaptoethanol (GIBCO-BRL, cell culture grade), and 21 mL of nutrient mixture that consists of 4 mM L-glutamine (GIBCO-BRL), sodium pyruvate (Sigma), nonessential

amino acids (Sigma), 10 U/mL Penicillin G (Sigma), and 150 µL/mL Streptomycin sulfate (Sigma).

2.1. b. Heat inactivation of fetal bovine serum

Fetal bovine serum (FBS) was heat inactivated to destroy the complement that may cause the induction of apoptosis. FBS was thawed slowly to 37 °C in a water bath with the occasional mixing of the contents. FBS was then transferred into 50-mL falcon test tubes, and the test tubes were placed into a 56 °C water bath for 30 minutes. Heating the serum for longer than 30 minutes or higher than 56 °C will have an adverse effect on the efficacy of serum. In order to prevent protein coagulation and ensure uniform heating, the serum was swirled every 10 minutes. The heat-inactivated serum was immediately cooled in an ice bath and stored at -20 °C for later use.

2.1. c. Cell storage and thawing for use

Cells were stored under liquid nitrogen. Four million cells were suspended in 1 mL of freeze medium that contained 90% heat inactivated fetal bovine serum and 10% of RPMI 1640 media. The cell suspensions were transferred to a cryovial that were kept at -70 °C overnight to prevent sudden shock to the cells. The cryovials were finally transferred to a liquid nitrogen tank for storage.

The cell suspension was thawed in a 37 ^{o}C water bath and then was transferred to a 15-mL falcon test tube for centrifugation. The frozen medium was aspirated and the cells were washed with a few milliliters of phosphate buffered saline. The cell suspension was centrifuged and the phosphate buffered saline was aspirated. The cell pellet was

resuspended in a few milliliters of media and transferred to a T-75 flask for further growth.

2.1.d Cell viability assay: Trypan blue exclusion assay

Performing a trypan blue exclusion assay assessed cell viability of myoblasts after treatment with pro and/or anti-oxidants. The cells were suspended in 30 µL of 0.4 % trypan blue stain (GIBCO-BRL) by repetitive pipetting. A 20-µL aliquot of the mixture was transferred to a hemocytometer slide. The total number of cells and the number of the stained cells (dead cells) were counted using a low power microscope. Dead cells stain blue, whereas live cells remain colorless. The percentage of cell death was calculated using the following equation:

% of cell death = (# of dead cells)/ (total # of cells) × 100 %.

2.2 GC-MS conditions

The standards and the cell samples were maintained in a gastight, temperature-regulated (37ºC) glass chambers within a small incubator assembly. The samples were analyzed by a cryofocusing system that interfaced with an HP 6890 gas chromatograph (Hewlett-Packard, Atlanta, GA) and a Leco Pegasus II time-of-flight mass spectrometer (LECO Corp., St. Joseph, MI), equipped with electron impact ionization and an electron multiplier detector. The GC column was an RTX-5, 30 m, 0.25 mm I.D., 0.25 µm film thickness (Restek Corp., Bellefonte, PA) and was maintained at 50 ºC for 30 s, then ramped at 30 ºCmin^{-1} to 80 ºC. High-purity hydrogen was used as the carrier gas after passage through a triple filter for the removal of hydrocarbons, oxygen, and water (Restek

Corp., Bellefonte PA). The transfer line to the mass spectrometer and the ion source temperature were maintained at 180 ºC. The detector was operated at 1700 V with a sampling rate of 30 spectra·s^{-1} and a solvent delay of 30 s.

Headspace samples were drawn via vacuum pump to a gas-cooled metal trap to rapidly preconcentrate gaseous sample. The inlet system is based on condensation (cryofocusing) of sample into a Cu / Ni alloy tube maintained at -90 °C. Samples are injected to the GC-TOFMS when the trap is resistively heated by a 90-V capacitive discharge. The peroxidation reactions were screened every ten minutes. In between each sample, blank measurements of room air were obtained in order to determine if crossover contamination was occurring. When switching solutions in the chamber, blanks were obtained after cleaning and prior to the addition of a new standard in order to validate cleanliness and prevent contamination.

2.3 Preparation of standards using PFB-derivatization method

The standards and the cell samples were prepared by the modified method originally developed by Liu et al [20]. The aldehydic moiety was converted to a derivative of pentafluorobenzyl hydroxylamine. 500 µL of the standards and the samples (after homogenization with 100 µL of 70% methanol) were suspended in 500 µL of 0.1 M sodium acetate, pH 6.0, and this was followed by the addition of 150 µL of O-(2,3,4,5,6-pentafluorobenzyl) hydroxylamine hydrochloride, followed by the addition of 100 µL of 0.1M pipes buffer. The samples were vortexed for 1 minute and left to stand for 10 minutes. Then 1mL of HPLC grade hexane was added and the samples were centrifuged

for 2 minutes at 5000 rpm. The process was repeated four times until the entire pentaflurobenzyl derivatives were extracted. The extracts were dried under nitrogen gas at 65˚c. After complete drying, 25 µL of anhydrous pyridine was added followed by 100 µL of N., O-bis (trimethylsilyl) trifluoroacetamide in 1% trimethylchlorosilane. The tubes were sealed and incubated at 65˚c for 1hour. The samples were then dried under nitrogen gas and finally resuspended in 70 µL of ethyl acetate before loading onto the GC.

2.4 LC -MS conditions (Varian instrument)

The 9-HTE samples were analyzed by a Varian 3800 gas chromatograph coupled to a Saturn 2200 mass spectrometer (Varian Corp.), equipped with electron impact ionization, chemical ionization, and an electron multiplier detector. The GC column was an RTX-5, 30 m, 0.25 mm I.D., 0.25 µm film thickness (Restek), and was maintained at 50 ºC for 2 min, then ramped at 20 ºCmin^{-1} to 280 ºC. High-purity hydrogen was used as the carrier gas after passage through filters for the removal of hydrocarbons, oxygen, and water. The transfer line to the mass spectrometer and the ion source temperature were maintained at 180 ºC. The 1177 automated injector (Varian Corp) was used for sample injections. The oven temperature was maintained at 250˚c. At times the samples were analyzed using 100% methanol as a liquid chemical reagent. Comparison experiments were done using both EI and CI methods.

2.5 Cell culture of 9-HTE cells

9-HTE cells were cultured in the same fashion as C2C12 cells.

2.5. a. Preparation of 9-HTE cells

9-HTE cells were seeded at a density of 2.0 X 10^6 cells.ml^{-1} of DMEM medium and the cells were incubated for 48 hours at 37ºC. Following a 48 hr of incubation, the DMEM media was replaced by a freshly prepared serum-free SABM (small airway cell basal medium), which contains no antimicrobial agents (SAGM from Clonetics, San Diego, Calif.), and allowed to grow overnight. The cells were treated with 1:100 of nontypeable *Haemophilus influenzae* (NTHi) bacteria (Clemans). After the addition of bacteria, the cells were derivatized at 0-, 2-, 4-, 8-, 12-, and 16-hour time periods using the PFB-Oxime derivatization method and analyzed by the LC-MS (Varian Corp). A control was also analyzed for every time period.

2.5. b. Culture of *Haemophilus influenzae* bacteria

The nontypeable *Haemophilus influenzae* (NTHi) bacteria were cultured on chocolate agar in 5% CO_2 at 37˚ C overnight and transferred to 10mL of levinthal broth (brain heart infusion broth supplemented with hemin (100 μg/mL) and NAD (20 μg/mL) and grown in 5 % CO_2 at 37˚ C overnight to stationary phase as followed by Clemens et al [40].

RESULTS

3. 1 Hexanal standard curve

Standard curves using GC-TOFMS for hexanal, 4hydroxynonenal, and malondialdehyde were obtained to determine the range over which these products could be quantified in cells. Figure 14 shows the calibration curve of hexanal. The x-axis shows hexanal concentration in micro molar, and y-axis shows the peak area; the curve is linear in the range from 2.59 μM to 41.5 μM. The correlation coefficient of the line encompassing the standard curve is 0.982. Figure 15 shows the chromatogram for the 24.9 μM hexanal standard. Hexanal elutes at about 78 secs, and the peak is characteristically asymmetrical under these conditions of the assay. The linear regression equation of this curve was used to calculate the concentration of hexanal in reaction samples from their corresponding peak area. The ions resulting from hexanal fragmentation include *m/z* 27, 39, 41, 43, 44, 56, 57, 72, and 82, and the peak areas for these ions were added to obtain the combined peak area for hexanal. The mass fragmentation spectrum of hexanal is shown in Figure 16.

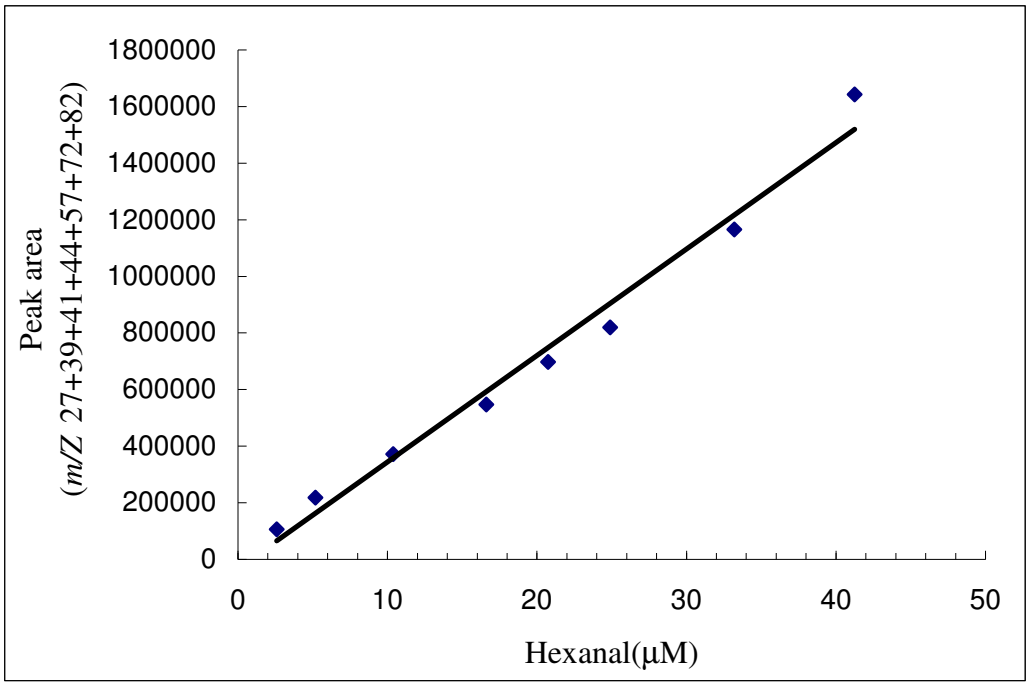

Figure 14. Hexanal calibration curve from 2.59 µM to 41.5 µM. The slope of the line is y = 310909x and the correlation coefficient, R^2 is 0.9824.

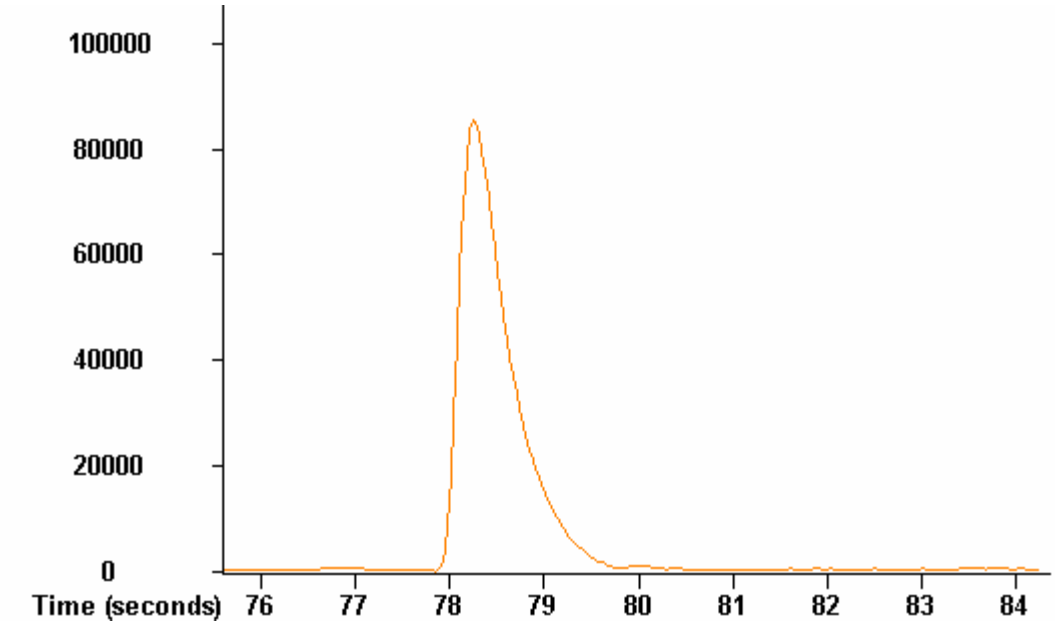

Figure 15. Chromatogram of 24.9 µM of Hexanal

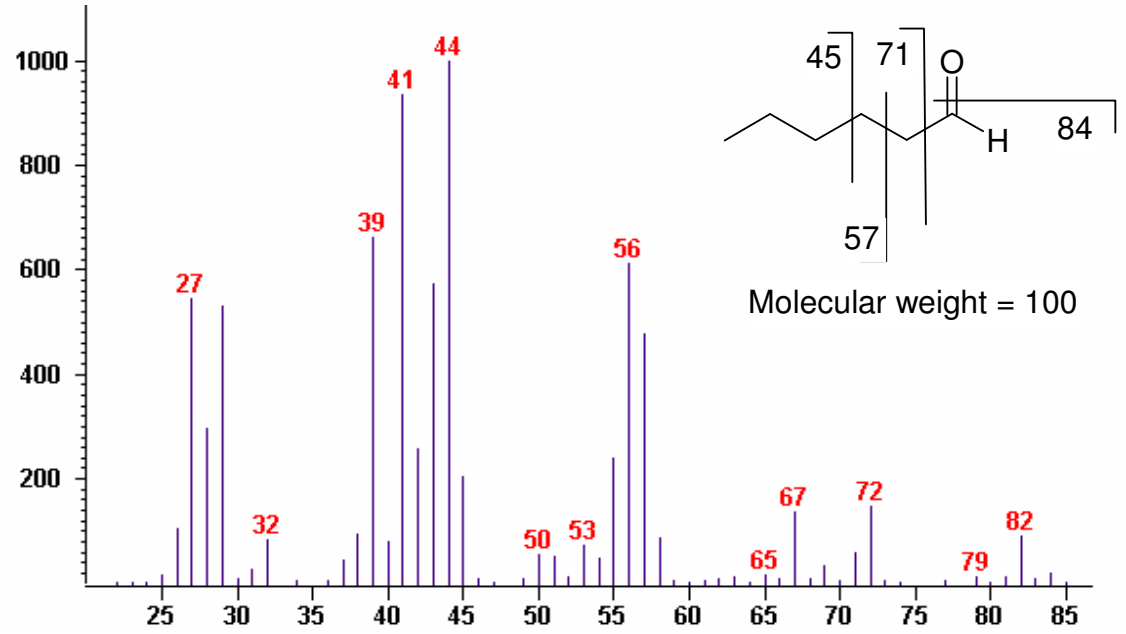

Figure 16. Mass fragmentation spectrum for 21.49 µM of hexanal. Shown in the inset is the putative breakage pattern of hexanal.

3. 2 Malondialdehyde (MDA) standard Curve

MDA calibration curve was developed using the modified PFB oxime derivatization procedure, and the derivatized samples were analyzed by GC-TOFMS. Figure 17 shows the calibration curve for MDA. The x-axis shows MDA concentration in µM, and y-axis shows the peak area. The curve is linear over a range from 0.5 to 8.0 µM, and the correlation coefficient of the curve is 0.9556. The linear regression equation of this curve was used to calculate the concentration of MDA produced in the cell samples from their corresponding peak areas. Figure 18 shows the chromatogram of the 0.5 uM MDA standard. Interestingly, there are at least three peaks associated with the MDA standard. The two incompletely resolved peaks are presumably the anti and syn conformers of the MDA derivative, whereas the peak between 350 and 353 secs is

presumably the PFB oxime derivative of glyoxal, a contaminant of MDA standard. The ions resulting from MDA fragmentation include *m/z* 181 and 250. Figure 19 shows the corresponding mass fragmentation spectrum. Mass fragments *m/z* 181 and 250 for the combined peak of the anti and syn conformers were used for detecting and quantifying MDA in the cell samples. The product formed as a result of derivatization and the possible origin of the 181 and 250 is shown in Figure 20.

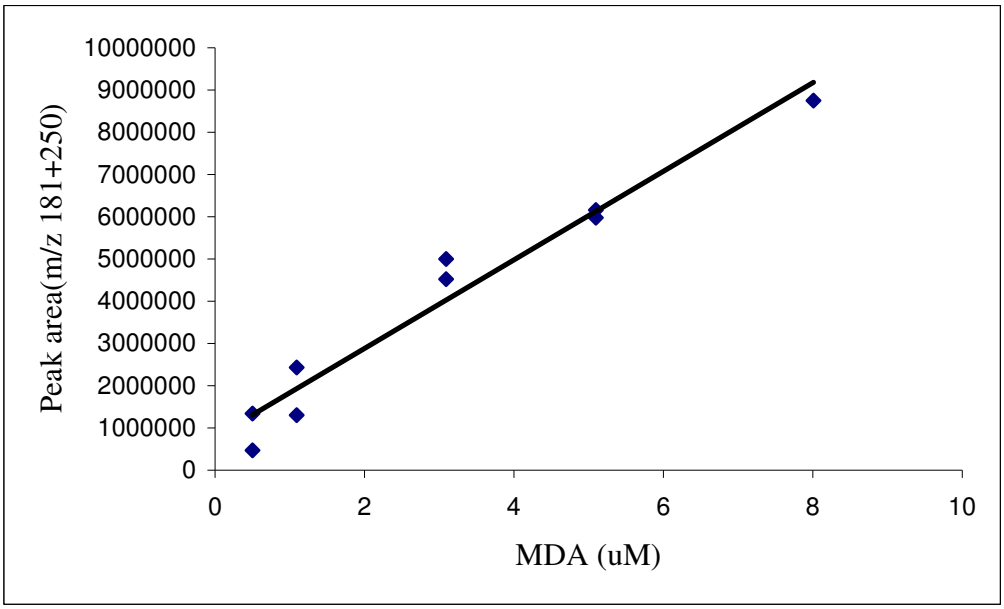

Figure 17. MDA calibration curve as determined by PFB oxime derivatization method from 0.5 to 8.0 µM. The slope of the line is y = 1E+06x and the correlation coefficient, R^2 is 0.9556.

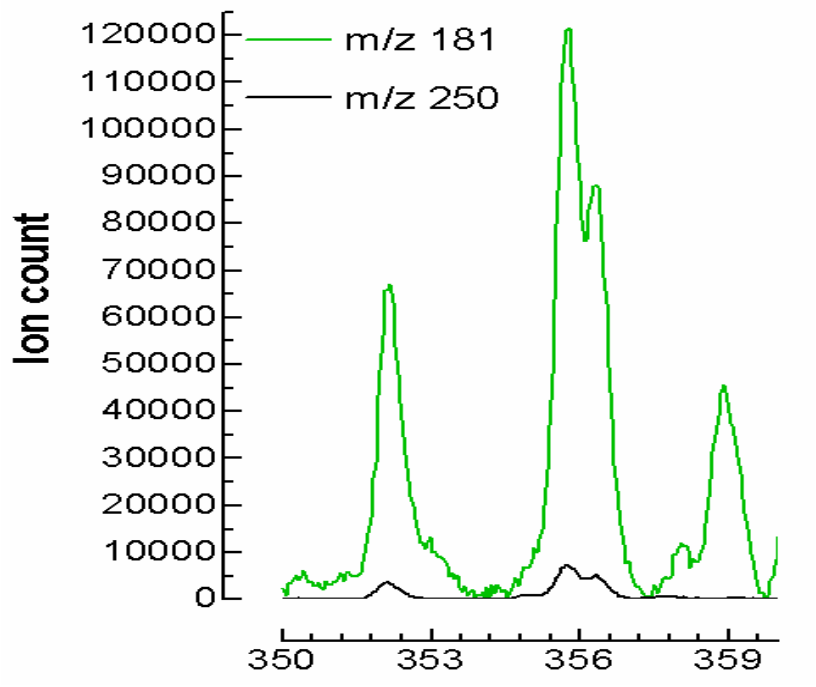

Figure 18. Chromatogram pattern of the 0.5 µM MDA standard.

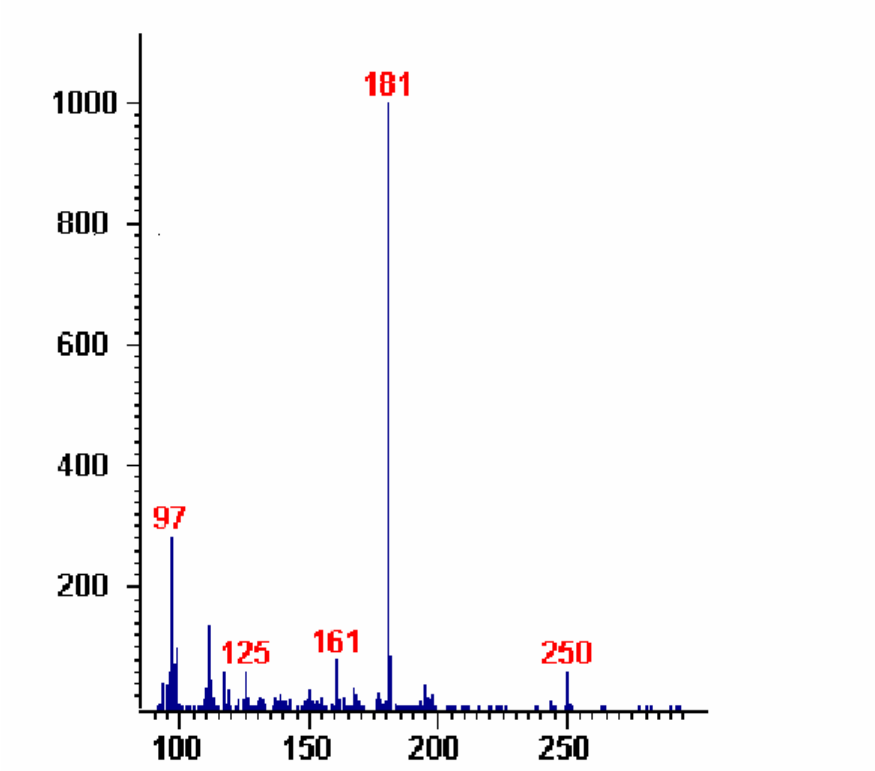

Figure 19. Mass fragmentation pattern of the 0.5 µM MDA standard.

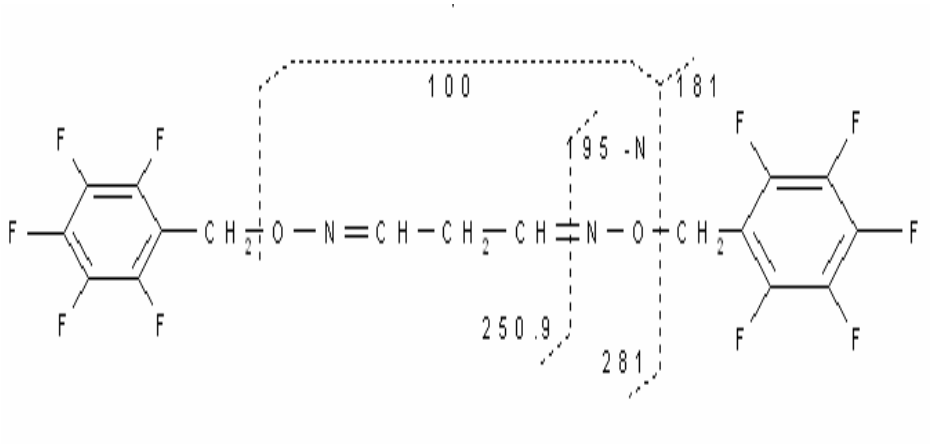

Figure 20. MDA-PFB derivatization product

3.3 4-HNE Calibration curve

The modified PFB oxime derivatization procedure was also followed to determine the 4-HNE calibration curve. Figure 21 shows the 4-HNE calibration curve in the range from 0.5 to 18 μM using 4-hydroxyhexenal as an internal standard. An internal standard was used for the correction of data due to variations in the extent of extraction of 4HNE and hence, 4HHE in the standards and samples and in the variation of the solvent in the assay vial due to evaporation. The x-axis of the standard curve shows 4-HNE concentrations in μM, and y-axis shows the peak area ratio of 4-HNE/4-HHE. A linear curve was obtained over a range of 0.5 uM to18 uM with a correlation coefficient of 0.962.

Mass fragments *m/z* 242 and 352 were used for detecting and quantifying 4-HNE. Figure 22 shows the chromatogram for 0.5 μM 4-HNE and 4HHE and shows the characteristic syn and anti isomers of 4-HNE oxime derivative. The corresponding mass spectrum resulting from fragmentation of PFB derivatized 4-HNE includes *m/z* 181, 242

and 352 was shown in Figure 23. These fragmentation ions were used to identify 4-HNE in the cell samples along with the 4HHE that was added to the sample during analysis.

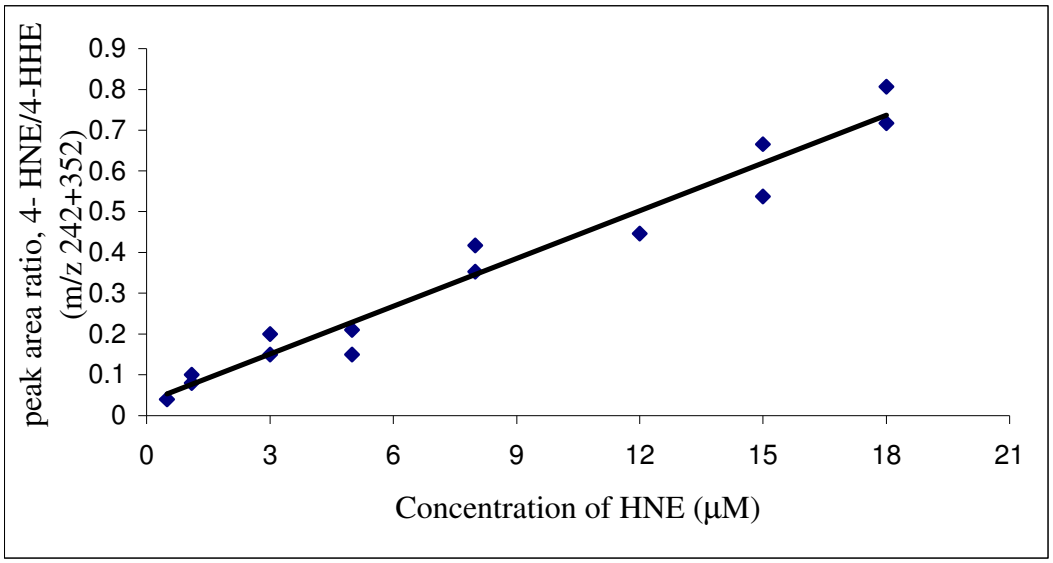

Figure 21. 4-HNE-calibration curve from 0.4 to 18 μM using 4-HHE as an internal standard as determined by PFB oxime derivatization method. The slope of the line is y = 0.039x and the correlation coefficient, R^2 is 0.962

The peak area ratio of the 4HNE ions 181, 242, and 352 to the 4HHE ions 181 and 352 was used to quantify the amount of 4HNE in samples. Figure 24 shows the product formed as a result of PFB derivatization and the putative cleavage pattern that gives rise to many of the ion fragments observed in the mass fragmentation pattern, including 181, 242, and 352 ions.

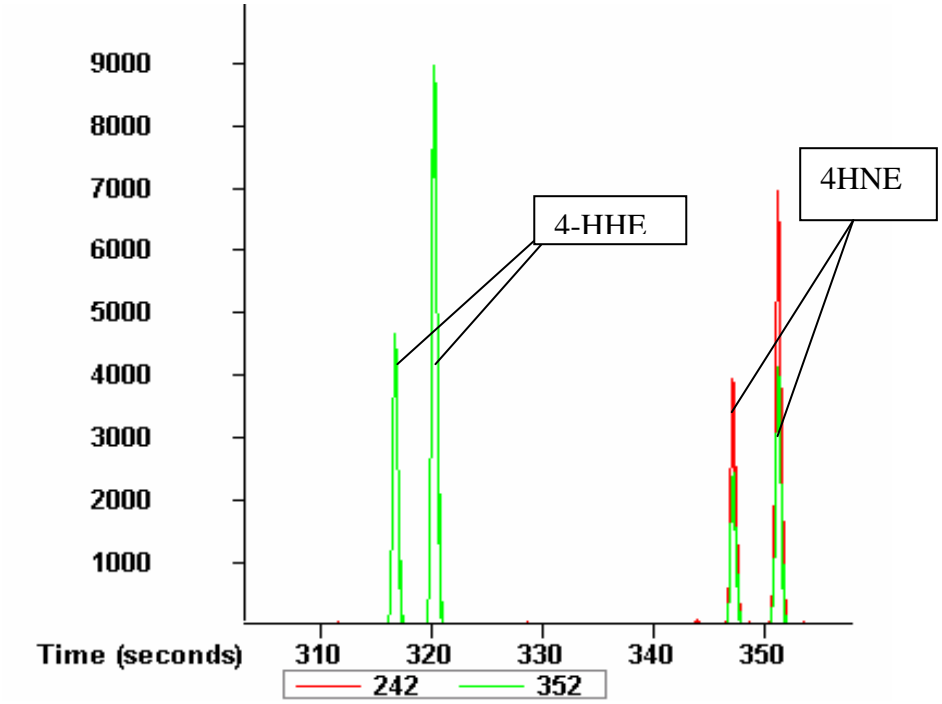

Figure 22. Chromatogram pattern of 18 µM of 4-HNE and 100 µM of 4-HHE

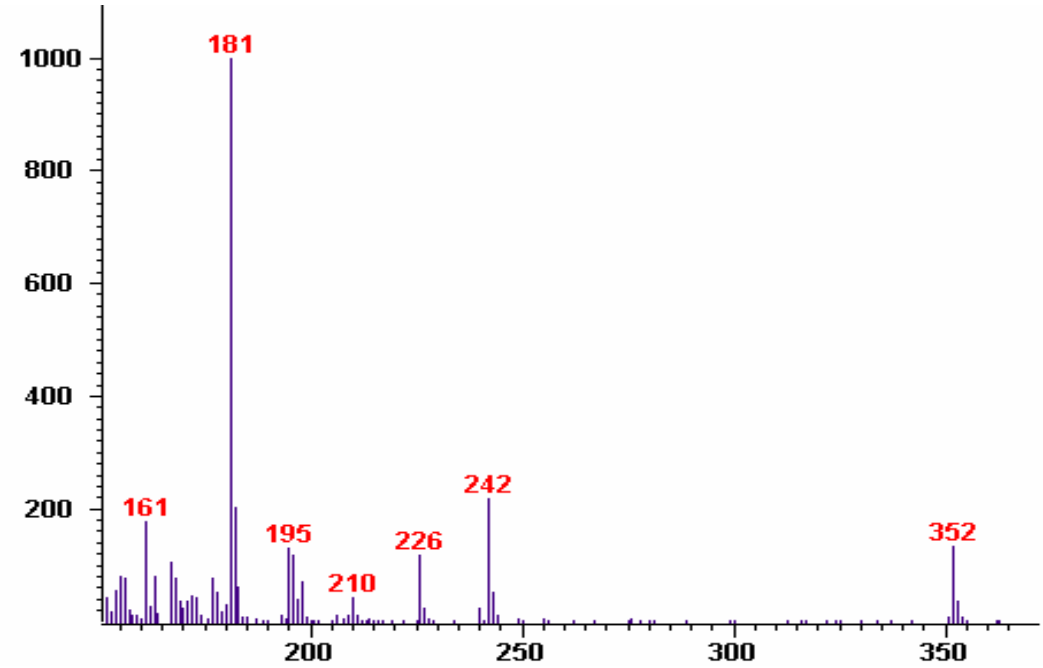

Figure 23. Mass fragmentation pattern of 0.5 μM 4-HNE

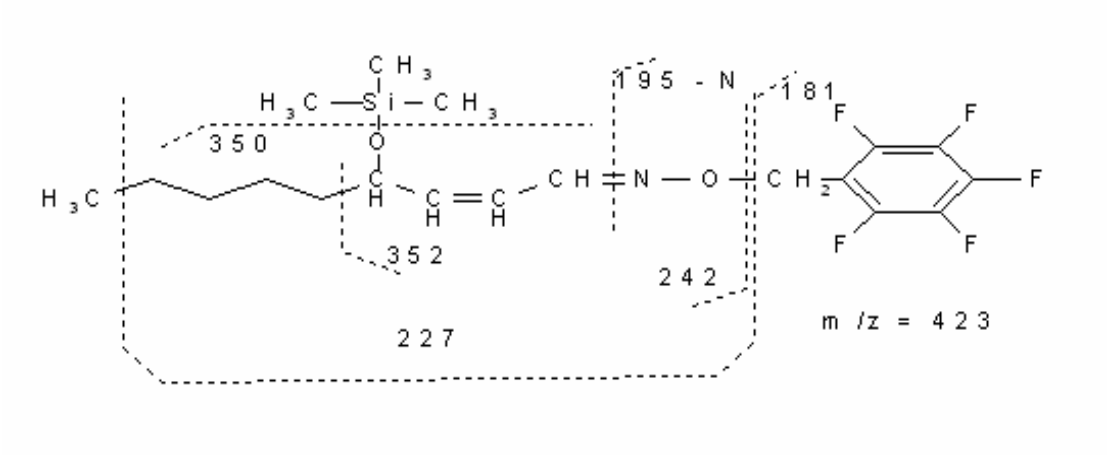

Figure 24. Putative fragmentation pattern of the 4-HNE-PFB derivative. The molecular ion m/z 423 is not observed under conditions of electron impact.

3.4 Formation of hexanal from C2C12 cells with and without prooxidant treatment

5 x 10^6 C2C12 cells/mL were incubated in cell chambers for 48 hrs at 37^o C to determine whether they produced any hexanal under conditions of normal growth and in the absence of any pro-oxidant stimulus. These represent the baseline conditions and were not expected to yield any hexanal. These samples were left in the incubation chamber for 10 minutes to equilibrate at 37 ^{o}C in a closed system, that is, the glass vial that is usually used in the analysis of oxygen concentration. After incubation these samples were analyzed by the GC-TOF/MS for identification of lipid peroxidation products over a 5-second period by removal of the headspace gas above the culture every ten minutes without disassembling the apparatus.

In the absence of a pro-oxidant, hexanal is first detected at 10 minutes, and increases steadily at a rather low rate over the subsequent 30 minutes. Companion

experiments were also done with 100 μM cumene hydroperoxide added after 10 minutes of incubation to determine if the pro-oxidant increases the rate of hexanal production, due presumably to stimulation of lipid peroxidation. The amount of hexanal formed was three times higher in the headspace of the cell culture treated with 100 μM cumene hydroperoxide when compared to background levels, although interestingly the rate of hexanal formation after the first ten minutes was not substantially different from background (Figure 25). The concentration was calculated from the linear regression equation obtained from the hexanal standard curve.

Figure 26 represents the chromatogram for hexanal obtained at the 20 min point. The fragmentation ions 44, 56, 67, 71, and 84, were used to identify the hexanal in the cell samples. The corresponding spectrum obtained from the cumene peroxide treated cells at 20 min time interval was shown in Figure 27. Further experiments were not pursued due to the disassembly of the cryofocusing apparatus used to collect and concentrate the headspace gas, so it is presently not understood whether any hexanal production could occur with this media alone in the absence of an oxidant or in the presence of a pro-oxidant. However, previous experiments performed with RPMI media containing the same amount of fetal bovine serum did not produce hexanal over a 60-min period at 37 ^{o}C in the same closed chamber (personal communication, Dr. Heather Holmes).

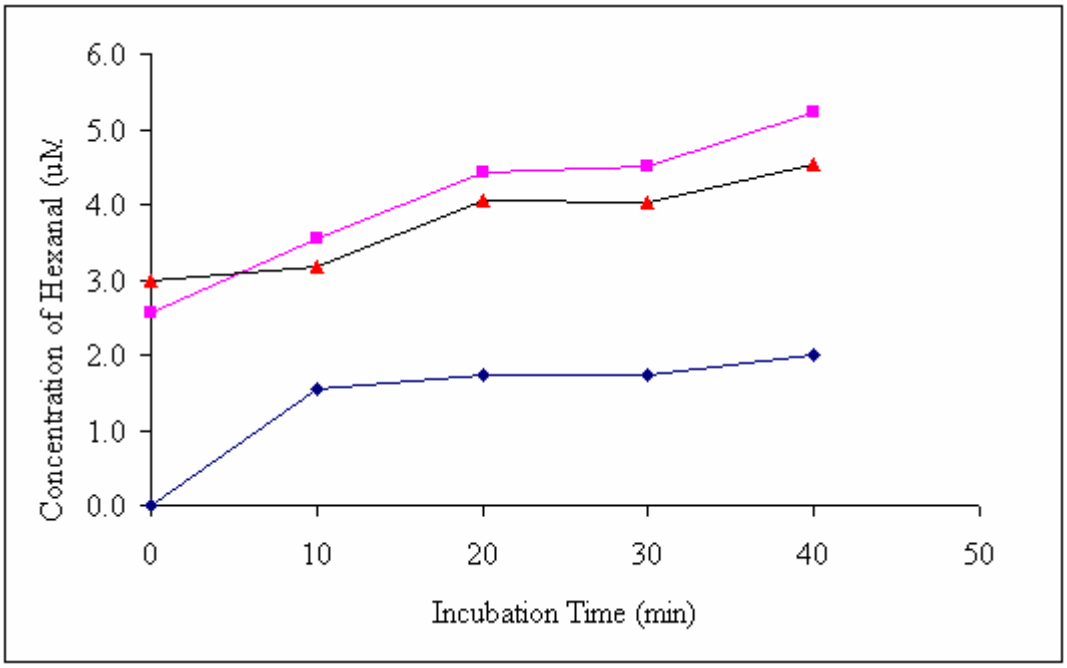

Figure 25. Hexanal production in C2C12 cells over time without any treatment (diamonds) and with 100uM cumene peroxide treatment (squares and triangles)

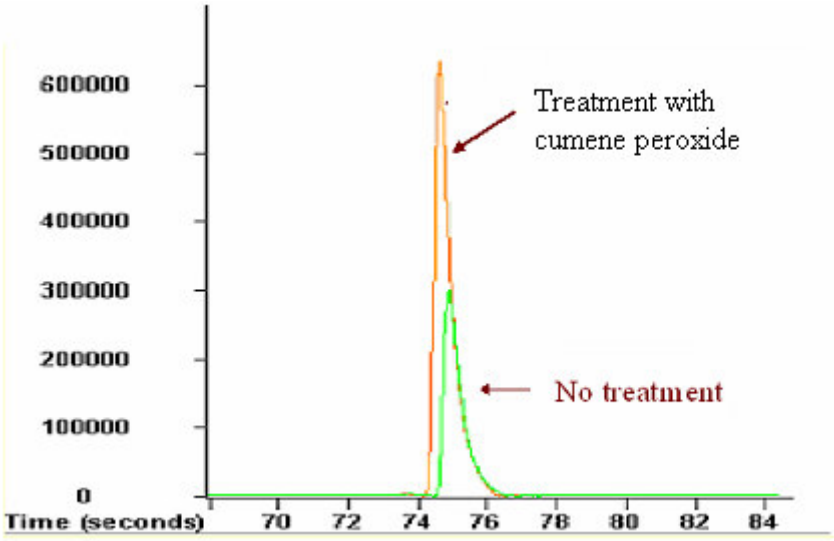

Figure 26. Chromatogram of the production of hexanal from C2C12 (treated and untreated) cells at 20 min point.

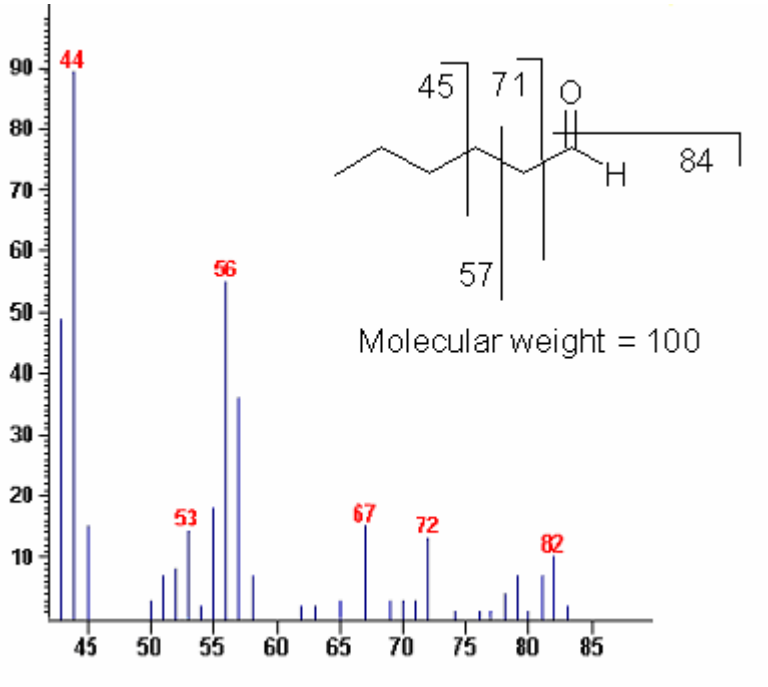

Figure 27. Spectrum obtained from the 100 µM cumene peroxide treated C2C12 cells at the 20 min time interval for the peak that co-migrates with hexanal standard.

3.5 C2C12 experiments using antioxidants

Experiments were also carried out to determine the effect of the treatment with a prooxidant, 100 µM cumene hydroperoxide, or an antioxidant, 1mM butylated hydroxyl toluene (BHT), after 30 min of incubation in the absence of these compounds. 5 X 10^6 C2C12 cells/mL were incubated for 48 hrs at 37^o C in cell chambers. The cells were incubated in an oxygen chamber vial for ten minutes to maintain the temperature. They were then analyzed for the volatile product hexanal using GC-TOF/MS in ten minute intervals. After 30 minutes the cells were treated with 100 µM cumene hydro peroxide or 1 mM butylated hydroxyl toluene. The results of this experiment are shown in Figure 28. The formation of hexanal after 1mM BHT treatment was much lower than after the

100 uM cumene hydroperoxide treatment. The concentration was calculated from the linear regression equation obtained from the hexanal standard curve.

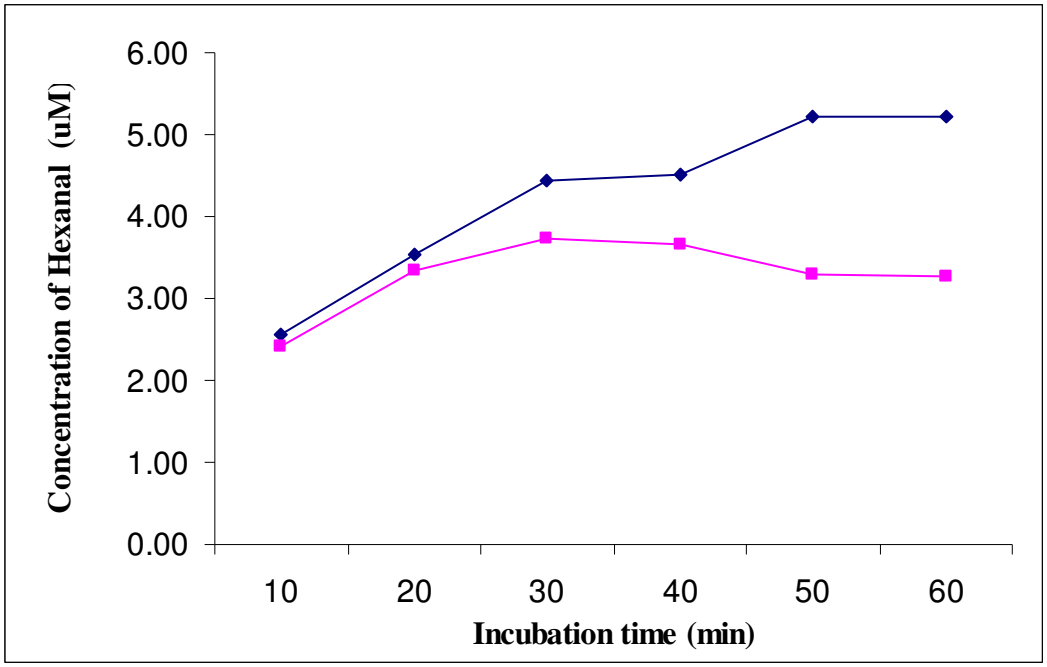

Figure 28. Formation of hexanal from C2C12 cells after treatment with 100 µM of cumene peroxide (Diamonds) or 1mM butylated hydroxyl toluene (squares) when added just prior to the analysis of the headspace at the 30 min time point.

3.6 Formation of malondialdehyde in C2C12 cells identified by GC-TOF/MS

2 X 10^6 cells/mL of mouse myoblast cells were incubated for 48 hrs at 37^o C. After incubation these cells were counted and found to have a cell density of 6 X 10^6 cells/mL. The aldehyde moieties of products in the cell samples were derivatized following the PFB oxime derivatization procedure. The samples were then analyzed by the GC-MS. Two well-resolved malondialdehyde peaks occurred around 356 secs. These peaks presumably represent the syn/anti congeners, each of which contained predominantly the 181 and the 250 ions as shown in Figure 29. The peak centered at

about 352 secs. has not been positively identified, although the mass fragmentation spectrum of the compound is similar to that of the PFB oxime derivative of glyoxal. The corresponding spectrum showing the fragmentation ions is shown in Figure 30.

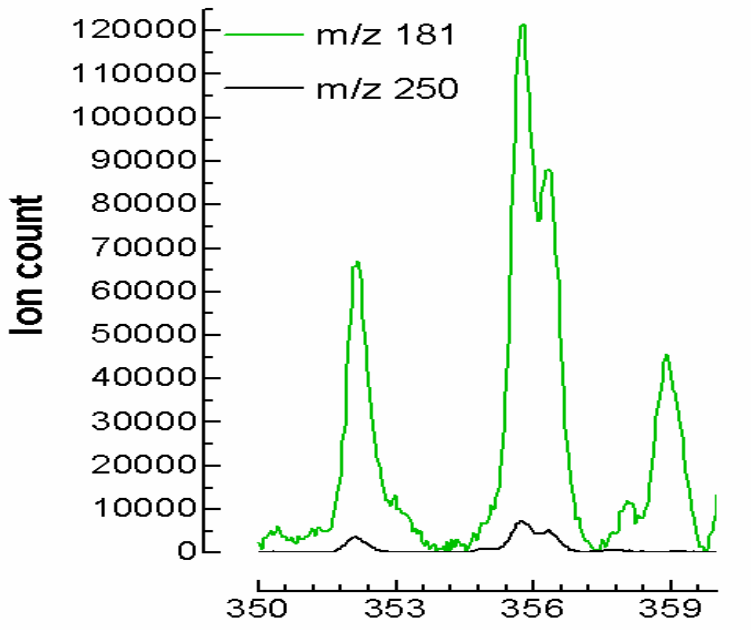

Figure 29. Chromatogram showing the formation of MDA from C2C12 cells

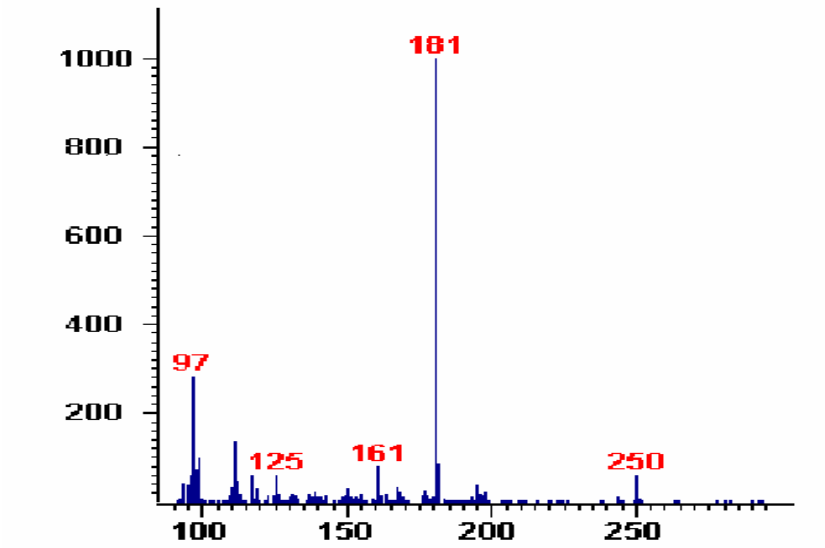

Figure 30. Spectrum showing the MDA fragmentation ions obtained from C2C12 cells

3.7 Formation of 4-HNE in C2C12 (myotubules) cells identified by GC-TOF/MS

Companion experiments were done using mature mouse myotubules (C2C12) cells. The cell samples were derivatized using the PFB oxime method. Interestingly, the cells did not show any formation of malondialdehyde, although a trace of another toxic product of lipid peroxidation, 4-HNE, was observed. The identification of HNE was made easier using an internal standard like 4-HHE. A tiny peak corresponding to 4-HNE was identified around 352 seconds. Two twin peaks were identified representing the syn and anti forms of 4-HNE and 4-HHE, corresponding to the 352+242 and the 352 ions, respectively. The chromatogram thus obtained is shown in Figure 31, and the corresponding spectrum showing the fragmentation ions is shown in Figure 32.

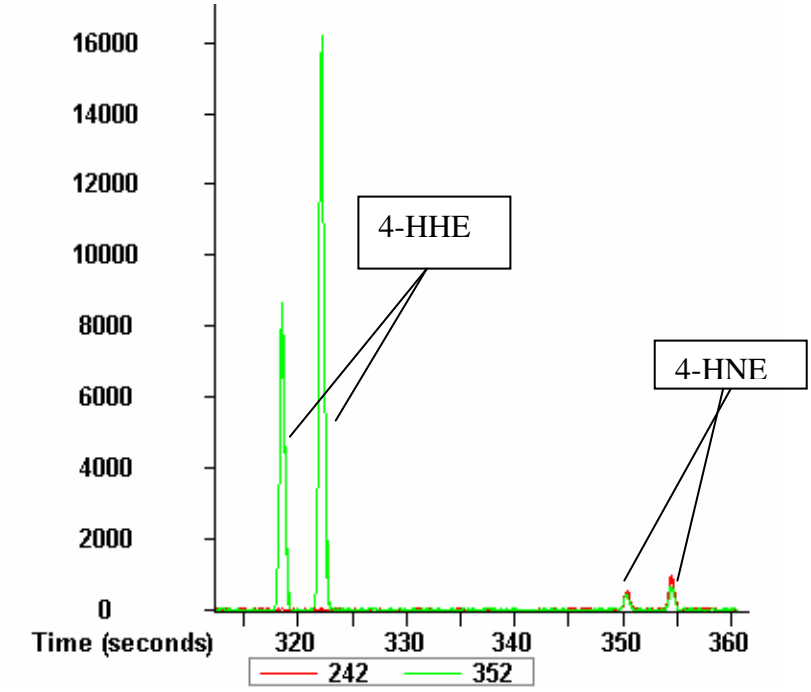

Figure 31. Chromatogram showing the formation of 4-HNE from mouse myotubules cells

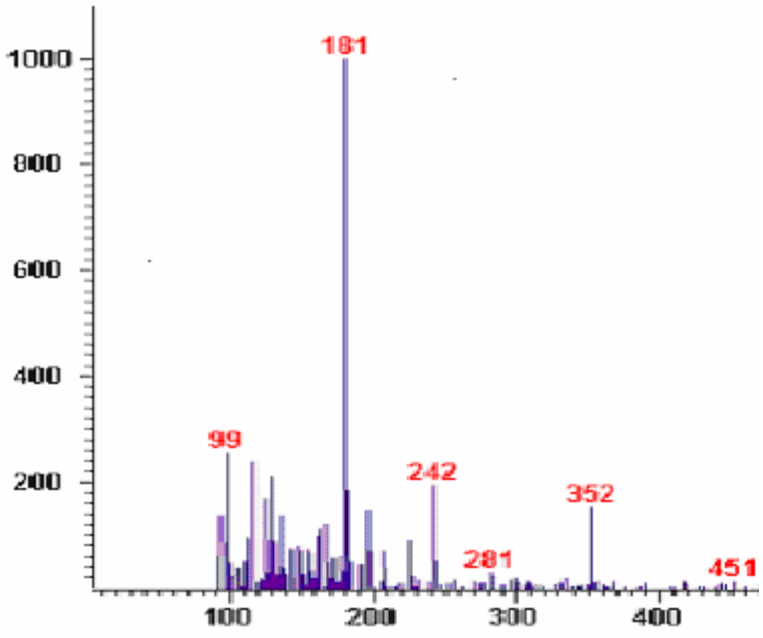

Figure 32. Spectrum showing the 4-HNE fragmentation ions obtained from C2C12 myotubule cells

3.8 Formation of Malondialdehyde in human tracheal epithelial cells (9-HTE)

Human tracheal epithelial cells (9-HTE) were seeded at a density of 2 x 10^6 cells/mL of DMEM media, and incubated for 48 hours at 37 ºC. Following 48 hr of incubation, the DMEM media, was replaced by a freshly prepared serum-free SABM (small airway cell basal medium), which contains no antimicrobial agents (SAGM from Clonetics, San Diego, Calif.), and allowed to grow overnight. The cells were treated with 1:100 of nontypeable *Haemophilus influenzae* (NTHi) bacteria. After the addition of bacteria, the cells samples were taken at 0-, 2-, 4-, 8-, 12- and 16-hr time periods, and the aldehydes were derivatized to form the PFB-oxime and analyzed by the GC-MS. A companion time course was done to determine the extent of formation of aldehydes in the epithelial in the absence of NTHi.

Figure 33 shows the pattern obtained by plotting time in hours on x-axis and the peak area obtained from the malondialdehyde (identification was based on the ions 181, 250, 463, 643) on the y-axis.

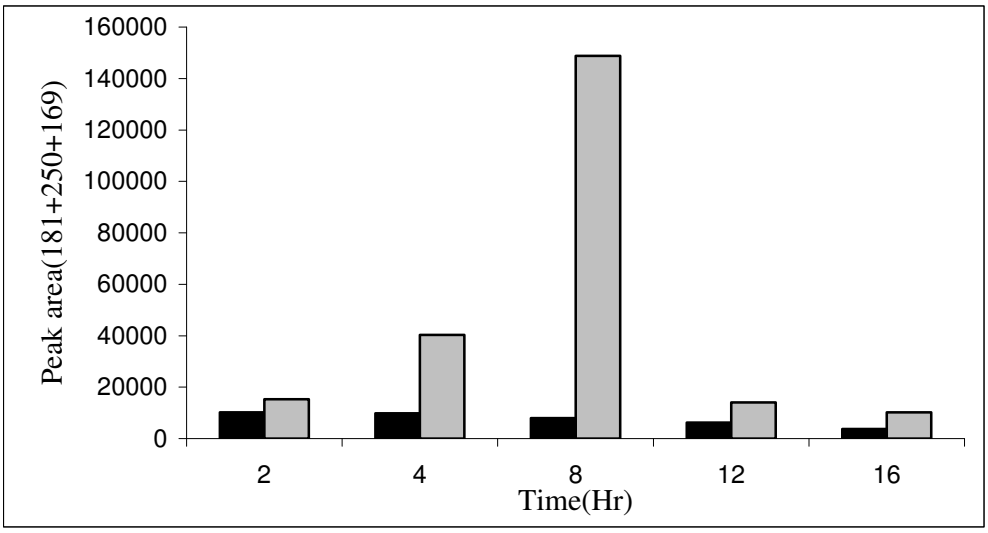

Figure 33. Formation of malondialdehyde in the *Haemophilus influenzae* treated 9-HTE cells. Control cells are shown in dark bars and 9-HTE cells treated with 1:100 bacterial cells are shown in grey bars.

Dark bars represent the control cells and grey bars represent the bacteria treated cells. The results showed that the amount of malondialdehyde production began to rise at 4hr time period with 8 hour time period reaching the maximum production, and finally there was a decrease in the formation at 12hr and 16 hr time period. The amount of malondialdehyde formation by the control cells was relatively constant throughout the experimental time.

Figure 34 represents the chromatogram obtained by the 9-HTE cells treated with *Haemophilus influenzae* (1:100) for an 8-hr time period. The x-axis shows time in minutes, and the y-axis shows the ion intensity. A malondialdehyde peak was noticed around 11.5 minutes. The corresponding spectrum thus obtained from the chromatogram is shown in Figure 35. Ions 181, 250, 463, and 643 were used to identify the malondialdehyde peak.

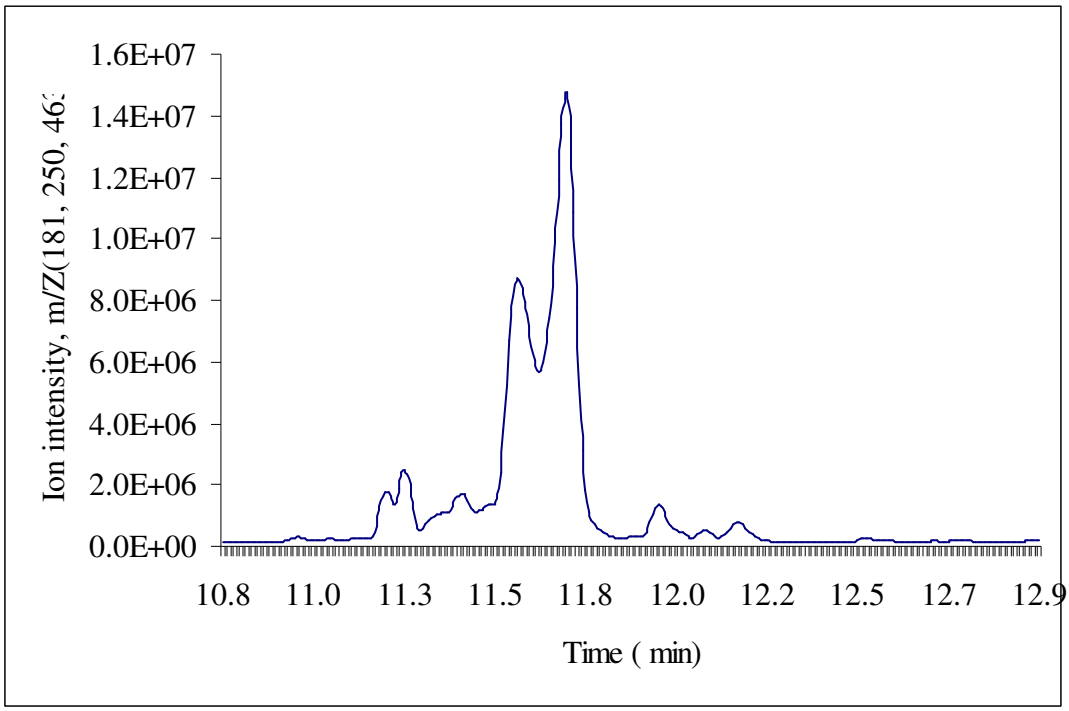

Figure 34. Chromatogram of the formation of malondialdehyde in the *Haemophilus influenzae* treated 9-HTE cells (8 hour treatment)

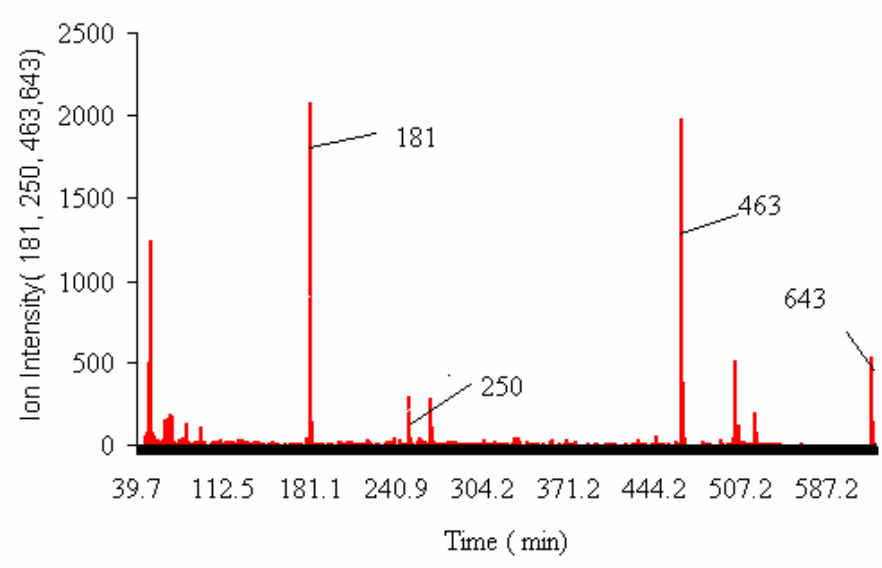

Figure 35. Spectrum of malondialdehyde from the *Haemophilus influenzae* treated 9-HTE cells (8 hour treatment)

3.9 Identification of novel aldehydic products of lipid peroxidation in the 9-HTE cells

Several unknown compounds corresponding to hydroxy aldehydes were also identified in the chromatograms based on their ion fragmentation pattern. Those results were treated as preliminary results, as commercially prepared standards for those identified hypothetical aldehydes were not available. Figure 36 shows a typical mass fragmentation pattern for an aldehyde. Figure 37 shows a sample spectrum showing fragmentation ions 181, 167, 195, obtained as a result of breakdown of aldehydes. These tentative aldehydes are noticed in most of the spectra and are tentatively identified as hydroxy aldehydes.

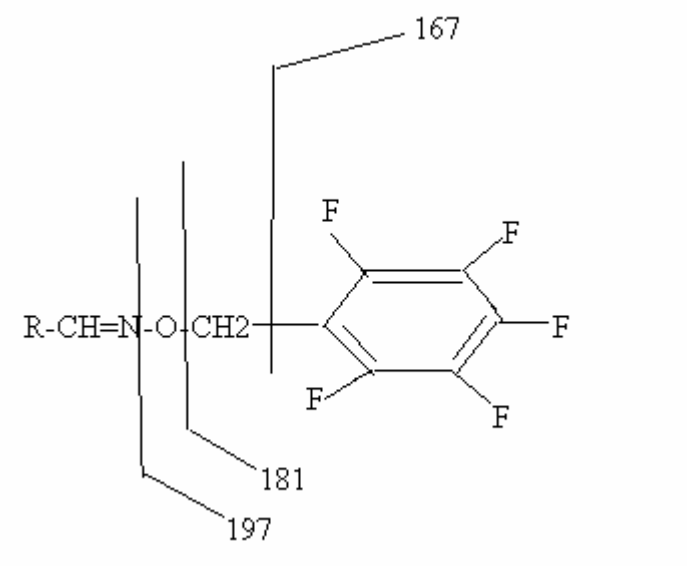

Figure 36. Aldehyde -PFB derivative fragmentation pattern

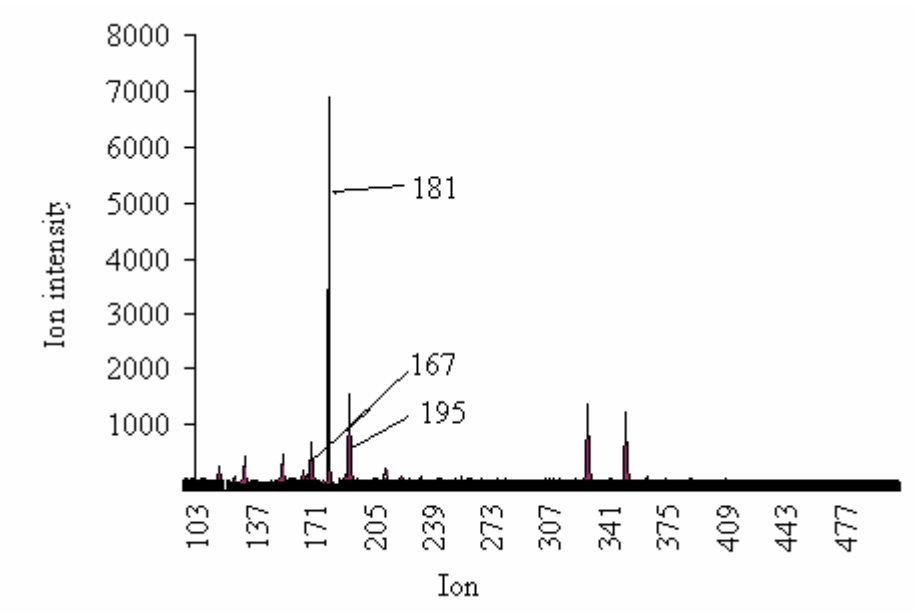

Figure 37. Typical mass fragmentation pattern of an aldehyde

DISCUSSION

Identification of the physiological, toxicological and pathological effects of aldehydic products of lipid peroxidation have necessitated the techniques that require their identification and quantification in biological materials. GC-MS is one of the useful methods for studying lipid peroxidation because of its high sensitivity and specificity [11]. MDA is one of the many aldehydic end products of lipid peroxidation, and hence the measurement of MDA by GC-MS reflects the formation and decomposition of lipid oxidation products. Whereas MDA constitutes a major metabolite of lipid peroxidation and the most frequently monitored, there are many other metabolites that may have diverse biological effects and that are only rarely studied. The purpose of this study was to ascertain the extent to which these products could be identified in animal cells. The use of the PFB ester method employed for the current study gave nanogram sensitivity for measuring lipid peroxides in biological tissues. Organic aldehydes tend to stick to protein and lipid amino groups by Schiff base linkages, and in the present study, hydroxylamine hydrochloride cleaved the Schiff base linkages and provided a very effective method for the extraction of these compounds from the cells.

The use of a miniature incubator with the GC-TOFMS facilitated the detection of hexanal, volatile product of lipid peroxidation in myoblasts, an undifferentiated form of muscle tissue. A rapid preconcentration of the sample was achieved as a result of using the cryofocusing inlet system as described by Amunugama et al. [41]. This method provided a very quick and nondestructive method for the analysis of hexanal both quantitatively and qualitatively. However, this method has a disadvantage with adherent

cell lines like the C2C12 myoblasts that adhere to the bottom of the flask; a clear estimation of the cell count is not possible. Interestingly, liquid phase extraction and derivatization and resolution of the aldehydes from myoblast cells indicated that malondialdehyde was easily identifiable, and no 4HNE was produced. Precisely the opposite pattern was observed for the myotubules, the fully differentiated form of the muscle cell in which no malondialdehyde was observed, whereas 4HNE was easily characterized. Usually, these two metabolites are produced in conjunction, and either is used to characterize lipid peroxidation *in vivo*. The results of the present study seem to stand in opposition to this belief. The source of these hydroxy alkenals and hexanal is presumably from the oxidation of the n-6 unsaturated fatty acids, arachidonic and linoleic acids, which are the major PUFAs in cells.

Inflammation associated with infectious diseases leads to the activation of neutrophils and endothelial cells that might promote lipid peroxidation [42]. In the current study, a model system was developed using the 9-HTE cells treated with *Haemophilus influenza* bacteria. Treatment of the bacteria showed elevated levels of malondialdehyde, an aldehydic product of lipid peroxidation at 8- hour incubation time interval. Parallel experiments were also done using the same cell model for the expression of Cox-1 enzyme, an enzyme responsible for the inflammation process (results not shown). Comparing the two results suggested that the products of lipid peroxidation are formed long before the COX-1 enzyme is activated. 4-HNE was not observed to be formed at any time period

Experiments carried out in the presence of serum in the media, however, showed elevated results of MDA, hence providing some evidence that the presence of serum in

the medium has exerted a positive effect on the levels of lipid peroxides and enhanced the results. A further analysis of the same experiment will answer these fundamental investigations.

Experiments were done to verify the efficacy of EI versus CI ionization methods for determining the lipid peroxidation, but not enough conclusions can be drawn based on the observed results, although CI gives a more detailed information regarding the ion breakdown and EI gives a better peak resolution. More experiments should be carried out to solidify the results.

Further experiments need to be carried out to ensure the formation of hydroxy alkenals in cell cultures. The derivatization procedure might need to be revised in order to analyze hydroxy alkenals. The aldehydes thus identified from the mammalian cell lines were easily quantifiable and are found to fit within the linear portion of the standard curve.

REFERENCES

1. Hein, M.; Best, L.; Pattison, S.; Arena, S.; *Introduction to General, Organic, and Biochemistry.* 6th edition. Brooks/Cole Publishing, 1997**,** 793-797.
2. Bettelheim, F.; Brown, W. H.; March J.; *Introduction to Organic & Biochemistry.* 4th edition. Harcourt College Publisher, 2001, 229
3. Murray RK, Granner DK, Mayes PA, Rodwell VW. Harper´s biochemistry. 25th edition Stamford, Connecticut: Appleton & Lange; 2000.
4. Lee, Y. J.; Je, H.j.; Kim, H.D.; Chung, W.S.; Zou, Y.; Kim, D.N.; Yoo, A.M.; Baik, S.H.; Yu, P.B.; and Chung, Y.H**.** *Eur. J. Biochem.* **2004**, *271*, 1339-1347.
5. Esterbauer, H.; Schaur, R.J.; Zollner, H. *Free Radic. Biol. Med.* **1991,** *11*, 81**–**128.
6. Kristal, B.S.; Park, B.K.; Yu, B.P. *J. Biol. Chem.* **1996**, *271*, 6033**–**6038.
7. Esterbauer, H.; Eckl, P.; Ortner, A. *Mutat. Res.* **1998**, *238*, 223-233.
8. Yeo, Helen C.; Helbock, H. J.; Chyu, D. W.; Ames, B. N. *Anal. Biochem.* **1994,** *220,* 391-396.
9. Marnett, L.J.; Hurd, H.K.; Hollestein, M.C.; Levin, D.E.; Esterbauer, H.; Ames, B.N. *Mutat. Res.* **1985**, *148*, 25-34.
10. Feron, V.J.; Til, H.P.; Cassee, F.R.; Van Bladersen, P.J. *Mutat. Res.* **1991**, *259*, 363-385.
11. Esterbauer, H. *Am. J. Clin. Nut.* **1993,** *57,*779S-785S.

12. Ceaser. E.K.; Moellering D.R.; Shiva. S.; Ramachandran. A.; Lander A.; Venkatraman A.; Crawford. J.; Patel. R.; Dickinson. D.A.; Ulasova. E.; Ji.S.; Darley Usmar. V.M. *Biochemical Society Transactions.* **2004,** *32,* 151-155.

13. Tapiero, H.; Ba, G.N.; Couvreur, P.; Tew, K.D. *Biomed. Pharmacother.* **2002**, *56*, 215–222.

14. Borgeat, P.*Can. J. Physiol. Pharmaco.* **1989**, *67*, 936–942.

15. Morrow, J.D.; Minton, T.A.; Roberts, L.J. *Prostaglandin.* **1992**, *44*, 155–163.

16. Moore, K.P.; Darley-Usmar, V.; Morrow, J.; Roberts, II, L.J. *Circ. Res.* **1995,** *77*, 335–341.

17. Banerjee, M.; Kang, K.H.; Morrow, J.D.; Roberts, L.J.; Newman, J.H. *Am. J. Physiol.* **1992**, *263*, H660–H663.

18. Moore, K.; Roberts, L. J. *Free Rad.* **1998,** *28*, 659-671.

19. Helblock, H.J.; Motchnik, P.A.; Ames, B.N. *Pediatrics,* **1993,** *91,* 83-87.

20. Liu, J., Yeo, C.H., Doniger, J.S., and Ames, N.B. *Analytical biochemistry* (1997), 245, 161-166.

21. Luo, P. X., Yazdanpanah, M., Bhooi, N., and lehotay, C.D. *Analytical biochemistry* (1995), 228, 294-298.

22. Banni, S.; Salgo, M.G.; Evans, R.W.; Corongiu, F.P.; Lombardi, B. *Carcinogenesis.* **1990,** *11,* 2053-2057.

23. Holley, A.E.; Slater, T.F. *Free Radical Res.Commun.***1991,** *15,* 51-63.

24. Tamura, H.; Shibamoto, T. *Lipid.* **1991,** *26,* 170-173.

25. Ebeler, S.E.; Hinrichs, S.H.; Clifford, A.J.; Shibamoto, T. *Anal.Biochem.* **1992,** *205*, 183-186.

26. Rosiers, C.D.; Rivest, M.J.; Boily, M.J.; Jette, M.; Carobe-Cohen, A.; Kumar, A. *Anal. Biochem.***1993,** *208,*161-170.

27. Cailleux, A.; Allain, P. *Free Radical Res. Commun.* **1993**, *18*, 323-327.

28. Sobotka, P.A.; Brottman, M.D.; Weitz, Z.; Birbaum, A.j.; Skosey, J.L.; Zarling, E.J. *Free Radical Biol. Med.* **1993**, *14*, 643-647.

29. Moore, K.; Roberts, L. J. *Free. Rad.* **1998,** *28*, 659-671.

30. Skoog, D. A.; Leary, J. J. *Principals of instrumental Analysis.* 4th edition. Saunders College Publishing, 1992**,** 583.

31. McNair, M.; Miller, J. M. *Basic Chromatography*; John Wiley & Sons Inc.: New York. 1998**.** 255-259.

32. Golary, M. J. E. *Gas Chromatography,* **1997**, Lansing symposium, Academic press, New York.

33. Venema, A. *J. High. Resolut. Chromatogr.* **1990,** *13*, 537.

34. Bianchi, A.; Varney, M. S.; Phillips, J. *J. Chromatogr.* **1999,** *467,* 111.

35. Frankel, E.N.; Hu, M. L.; Tappel, A. L. *Lipids.* **1999,** *24*, 976-980.

36. Stanshenko, E. E.; Puertas, A. M.; Martinez, J. R. *J. Bioanal. Chem.* **2002,** *373*, 70-74.

37. http://www.abcbodybuilding.com/magazine03/freeradicals.htm

38. Adams, A.K.; Best, M.T. T*he physician and sports medicine*. **2002,** 10.

39. Stentz, B.F, Umpierrez, E.G, Cuervo, R.; Kitabchi, E.A. *diabetes,* **2004,** 53, 2079-2086.

40. Clemans, L.D, Bauer, J.R, Hanson, A. J, Hobbs, V.M, ST. Geme III, W.J, Marrs, F.C.; Gilsdorf, R.J. *Infection and immunity.***2000,** 68, 4430-4440.

41. Amunugama, M, Clifford, C.D, Gutman, P.M, Soltani, M, Karunaratne, S, venkatachalam, K, Pernecky, S.J, Holmes, H.L.S.*Chromatographia,* **2004**, 60, 441-447.

42. Khair, O.A, Davies, J.R, Devalia, L.J. *European respiratory journal,* **1996**, 9, 1913-1922.